Title
Riffle-pool maintenance and flow convergence routing observed on a large gravel-bed river

Journal
Geomorphology, 114(3)

ISSN
0169-555X

Authors
Sawyer, April M
Pasternack, Gregory B
Moir, Hamish J
et al.

Publication Date
2010

DOI
10.1016/j.geomorph.2009.06.021

Title Riffle-pool maintenance and flow convergence routing observed on a large gravel-bed river

Running title: Riffle-pool maintenance observed

April M. Sawyer[a], Gregory B. Pasternack[a*], Hamish J. Moir[b], and Aaron A. Fulton[a]

Addresses:

[a]Department of Land, Air, and Water Resources, University of California, One Shields Avenue, Davis, CA 95616-8626, USA

[b]Macaulay Institute, Craigiebuckler, Aberdeen, Scotland AB15 8QH, UK

*Corresponding author. Tel.: +1 530-754-9243; Fax: +1 530-752-5262;
E-mail: gpast@ucdavis.edu.

Cite as: Sawyer, A. M., Pasternack, G. B., Moir, H. J., Fulton, A. A. 2010. Riffle-Pool Maintenance and Flow Convergence Routing Confirmed on a Large Gravel Bed River. Geomorphology 114:143-160, DOI: 10.1016/j.geomorph.2009.06.021

Abstract

Geomorphologists have studied and debated over the processes responsible for natural riffle-pool maintenance for decades. Most studies have focused on small wadable rivers, but they lack much description of overbank flood conditions or a spatially explicit characterization of morphodynamics. In this study, 1-m horizontal resolution digital elevation models were collected from a riffle-pool-run sequence before and after an overbank flood with a 7.7-year recurrence interval on the relatively large gravel-bed lower Yuba River, California. Digital elevation model differencing was used to quantify the magnitude and pattern of flood-induced morphodynamic change. Cross section based analysis and two dimensional hydrodynamic modeling of flows ranging from 0.147-7.63 times bankful discharge were completed to evaluate the hydraulic mechanisms responsible for the observed topographic changes. One key finding was that riffle-pool relief increased by 0.42 m, confirming the occurrence of natural hydrogeomorphic maintenance. Spatially complex patterns of scour and deposition exceeding 0.15 m at the scale of subwidth morphological units were reasonably predicted by the two dimensional mechanistic model that accounts for convective acceleration. The one dimensional cross section based method underperformed the two-dimensional model significantly. Consequently, multiple scales of channel nonuniformity and a dynamic flow regime caused the observed maintenance of the pool-riffle morphology through the mechanism of "flow convergence routing" proposed by MacWilliams et al. (2006).

Keywords: velocity reversal; pool-riffle sequence; hydrodynamic modeling; channel change; fluvial geomorphology

1. Introduction

Riffle-pool sequences are important morphological characteristics of low to moderate gradient gravel-bed streams. Local flow convergence and divergence in either freely formed (i.e., cross channel flow or sediment transport) or forced (i.e., channel bends, obstructions) channel patterns form such sequences (Lisle, 1986; Montgomery and Buffington, 1997). Pools are topographic depressions covered with finer sediment, while riffles are topographic highs covered with coarser bed material; these two features are defined relative to each other (O'Neill and Abrahams, 1984; Montgomery and Buffington, 1997). Under low-flow conditions, vertical variations in topography along the length of a river control hydraulics and sediment transport; pools having slow, divergent flow, low water-surface slope, and low transport competence; and riffles having faster, convergent flow, steep water-surface slope, and moderate transport competence (Clifford and Richards, 1992). Riffle-pool morphology creates physical heterogeneity, promoting habitat diversity for instream species (Gorman and Karr, 1978; Brown and Brown, 1984; Palmer et al.,1997; Giller and Malmqvist, 1998; Woodsmith and Hassan, 2005).

Explanations for riffle-pool sequence maintenance have been debated for decades. Geomorphologists historically observed a reversal in mean flow parameters (e.g., mean velocity, near-bed velocity, and bed shear stress) as a possible explanation for riffle-pool maintenance in gravel-bed rivers. The velocity reversal hypothesis states that "at low flow the bottom velocity is less in the pool than in the adjacent riffles" and that "with increasing discharge the bottom velocity in pools increases faster than in riffles" (Keller, 1971, p. 754). Gilbert (1914) first described a reversal in bottom velocity but was unable to quantify this observation. Lane and

Borland (1954) later speculated that channel hydraulic conditions in riffle-pool sequences and channel geometry both affect scour and deposition patterns during high flow events. Actual velocity measurements were not taken to support these observations until Keller's (1969, 1971) studies on Dry Creek near Winters, California. Keller measured near-bed velocities at pool and riffle cross sections during several safely wadable discharges. He showed that velocities became similar as flow increased, but not that the near-bed velocity in the pool actually became higher than in the riffle. Thus, he coined the "hypothesis of velocity reversal" (Clifford and Richards, 1992; MacWilliams et al., 2006).

The velocity reversal hypothesis has been highly contentious in the scientific community. Uncertainty mainly arises from differing approaches to describing this phenomenon (Woodsmith and Hassan, 2005). Early studies, such as Teleki (1971) and Whittaker and Jaeggi (1982), refuted Keller's velocity reversal hypothesis because of inconsistency with hydraulic principles and insufficient description of water-sediment interface conditions. Other studies aimed to describe the velocity reversal hypothesis using alternative parameters, such as mean boundary shear stress (Lisle, 1979), section-averaged velocity (Clifford and Richards, 1992; Keller and Florsheim, 1993) and section-averaged shear velocity (Carling, 1991).

Increasingly, field-validated hydrodynamic models are being used to describe and evaluate hydraulic and geomorphic phenomena (Keller and Florsheim, 1993; MacWilliams et al., 2006; Pasternack et al., 2008). Complete morphodynamic models that simulate mass and momentum conservation of water and sediment in dynamic gravel-bed rivers would be ideal, but they have not been widely used and validated yet. Simplified morphodynamic models that ignore momentum conservation violate observed interdependencies between depth and velocity as a function of stage in rivers and are not accurate enough for the questions under investigation.

Conversely, significant limitations have been reported when only semi-analytical equations or one-dimensional (1D) hydraulic models are used to evaluate gravel-bed river dynamics, because these tools do not incorporate necessary hydrodynamic mechanisms (MacWilliams et al., 2006; Brown and Pasternack, 2008b). It has been posited that two-dimensional (2D) and three-dimensional (3D) models yield a compromise at this time between the two unsatisfactory endmembers in that they enable spatially detailed characterization of velocity and bed shear stress at high flows under which field measurements are impractical. In one such study, MacWilliams et al. (2006) were able to determine that the velocity reversal hypothesis was not adequate to describe processes responsible for riffle-pool maintenance on Dry Creek in a reexamination of Keller's original study using 2D and 3D models. Instead of rejecting Keller's (1969, 1971) ideas, they proposed the concept of flow convergence routing as a "new working hypothesis" to describe these processes. It states that flow converges in riffles at low flows, causing armoring, gradual incision, and diminishing relief; but that during high magnitude, infrequent floods, flow converges in pools, causing rapid scour that enhances relief. MacWilliams et al. (2006) also reviewed all studies of velocity reversal (incorporating a range of flow parameters) and stated that these should be viewed as a "suite of multiple working hypotheses for explaining riffle-pool morphology" based on different maintenance mechanisms present in varying channel conditions. In this study, the flow convergence routing hypothesis is further explored in conjunction with the velocity reversal hypothesis to qualify riffle-pool maintenance mechanisms in a large, dynamic gravel-bed river system.

A key gap in the existing knowledge of riffle-pool maintenance is the lack of studies in larger gravel-bed rivers, defined as those with a nondimensional base-flow width to median bed material size ratio > 10^3 and a width too large to be spanned by the length of a fallen riparian tree. Most previous studies sought to observe pool and riffle hydraulics over a wide range of flows. This necessitates safe and practical wading conditions or a narrow channel that can be spanned by a simple bridge for measuring hydraulic variables during floods (e.g., Keller, 1969, 1971; Richards, 1976a,b; Clifford and Richards, 1992), and therefore previous efforts have focused on relatively small streams. In small streams, wood, boulders, and bedrock outcrops often create channel constrictions and significantly alter channel hydraulics in small streams (Thompson et al., 1998, 1999). In such circumstances, pool geometry is controlled by constrictions where flow and sediment convergence encourages scour and pool maintenance, while exit slopes control deposition at the pool tail (Thompson et al., 1998). However, such localized features' impact on large gravel-bed rivers is unknown.

The overall goal of this study was to address this critical research gap by investigating the mechanisms of natural riffle-pool maintenance on a large river meeting the above criteria. Two key elements enabled the characterization of riffle-pool response on a large river to an infrequent flood: (i) a uniquely managed river basin (as described in section 2) in a Mediterranean climate in a water year with two long periods of low flow punctuated by a single high-magnitude, short duration flood that enabled detailed pre- and post-flood channel characterization and (ii) a pairing of field observation and high-resolution 2D hydrodynamic modeling that simulated the effect of vertical and lateral channel nonuniformity on bed scour during the peak of the flood. 2D models have limitations as set forth below, but they can be used to explore hydrodynamic mechanisms beyond what is possible from empirical equations or simpler 1D models.

The specific objectives of this study were to (i) measure channel change at an ecologically important riffle-pool unit on a large dynamic river before and after an overbank flood and determine if relief was maintained; (ii) quantify riffle-pool reversals in point-scale depth-averaged velocity and bed shear stress as well as section-averages of those variables; (iii) compare the abilities of one-dimensional cross section based hydraulic geometry analyses and 2D hydrodynamic modeling to predict channel conditions such as width, depth, velocity, and discharge-slope relations- these are two different analysis tools used by different groups of practitioners, so it was helpful to use both to see what they reveal and then intercompare their findings; (iv) relate the observed pattern of scour and deposition caused by the flood to nondimensional shear stress predictions provided by a 2D hydrodynamic model and (v) reassess whether the flow convergence routing hypothesis was suitable to describe processes responsible for riffle-pool morphology maintenance for a large river. By combining observational field data, cross section analyses, and mechanistic modeling, obtaining a new and unique perspective on riffle-pool maintenance for large rivers was possible. Although this study does not end discussion about natural riffle-pool maintenance, it supported evidence of flow convergence routing and geomorphic significance in a large gravel-bed river for the first time.

2. Study Area

The Yuba River basin (California) flows SW on the western slope of the Sierra Nevada in northern California and drains a 3490-km^2 watershed in Sierra, Placer, Yuba and Nevada counties (Fig. 1). The North, Middle, and South Forks of the Yuba River converge in a canyon above Englebright Dam; and then Deer Creek, a sizable regulated tributary draining ~ 220 km^2, joins the Yuba ~ 1.9 km downstream in the canyon.

During the California Gold Rush (mid to late 1800's) gold-bearing Tertiary sediments were hydraulically mined after in-channel deposits were exhausted. As a result of hydraulic mining, mercury-laden hydraulic mine tailings from tributaries substantially increased the sediment supply to the Yuba River. Before hydraulic mining, hillslope erosion naturally dominated sediment production (James, 2005). According to Gilbert (1917), unlicensed hydraulic mining supplied ~ 522 million m^3 of sediment to the Yuba River until the Sawyer Decision of 1884 ended such large-scale operations (Curtis et al., 2005).

Englebright Dam (storage capacity of 82.6 million m^3) was built in 1941 as a debris barrier on the main stem Lower Yuba River (LYR). In 1971, New Bullards Bar Reservoir (storage capacity of 1.19 billion m^3) was completed at a site ~ 28 km upstream from Englebright on the North Fork Yuba River. Given that the Middle and South Forks do not have large reservoirs, large winter rainstorms and spring snowmelt commonly produce uncontrolled floods that overtop Englebright. Historically, large natural interannual variations in discharge occurred (Fig. 2), with rapid flow fluctuations in November through March from direct storm runoff, a sustained snowmelt flow from April through June, and a stable summer base flow from July to October (LYRFTWG, 2005). Streamflow data are recorded at the U.S. Geological Survey (USGS) Smartville gage (#11418000) 0.5 km downstream from Englebright Dam in the bedrock canyon. During the period between the completion of Englebright Dam in 1942 and New Bullards Bar in 1971, the statistical bankful discharge (Q_b, 1.5-year recurrence interval) at the Smartville gage was 328.5 m^3s^{-1}. In the period since 1971, the gage's Q_b is 159.2 m^3s^{-1}.

Present-day channel conditions are governed by past and present human activities. Dams, bank alteration, and in-channel mining often cause narrowing, incision, changes to channel pattern, and coarsening of bed sediments as a result of sediment supply reduction and increased transport capacity (Williams and Wolman, 1984; Kondolf, 1997). Even though Englebright Dam blocks all bedload replenishment to the LYR, high sediment supply–a legacy of hydraulic mining– means that the LYR remains a wandering gravel-bed river with a valley-wide active zone. However, the absence of a bedload influx contributes to a rapid valley-wide incision rate on the order of ~ 10 m over 65 years. Based on a comparison of photographs taken by G. K. Gilbert in 1906 and a series of aerial and ground-based photographs taken from 1937 to 2006 (White, 2008), a sequence of pools and riffles has persisted for decades despite the rapid rate of long-term incision (Fig. 3). Other historical channel changes in the LYR include significant anthropogenic bank and meander bend stabilization with large dredger tailing piles, channel activation and abandonment, riparian vegetation growth cycles, and natural levee stabilization. In summary, the geomorphology of the modern LYR is heavily impacted, but an abundant supply of coarse bed material and relatively natural flow regime (especially bedload-mobilizing flood flows) enabled riffle-pool sequence maintenance in the same locations for 30-100 years. A description of ecological conditions in the LYR, including details about the study site, is beyond the scope of this paper (see Moir and Pasternack (2008) and Pasternack (2008)).

2.1. Timbuctoo Bend study site

Downstream from Englebright Dam after the bedrock canyon ends, a valley-wide wandering gravel-bed river exists (Fig. 1). This study focuses on a ~ 450-m-long by ~ 200-m-wide riffle-pool-run unit of the LYR 6.25 river-km downstream from Englebright Dam at the apex of a large meander bend in the valley called "Timbuctoo Bend" (39°13'56" N., 121°18'48" W.). Timbuctoo Bend is characterized by active gravel bars, a well-connected floodplain, secondary and tertiary flood channels, and nonuniform channel geometry. Specifically, the study site has a large and dynamic island/bar complex that defines a riffle-pool-run morphology (upstream to downstream). Below Q_b, a perennial side channel existed along the river-right bank of the study site; above Q_b the island and part of the floodplain are submerged. The bankful channel in 2004 and 2005 was defined by moderately steep alluvial banks lined by nonencroaching, semipermanent, low-growing woody riparian vegetation (mostly *Salix spp.*) (LYRFTWG, 2005). At ~ $2 \cdot Q_b$ locations with valley-wide flow exist, and then at ~ $3\text{-}4 \cdot Q_b$ valley-wide flow existed across the entire site. Isolated, streamlined bedrock outcrops with localized scour holes exist on both sides of the valley in the study area. According to Moir and Pasternack (2008), the bed material at the site was a gravel and cobble mixture (D_{50} of 60 mm and D_{90} of 123 mm) with very little sand present near the bed surface and a heavily armored riffle crest. The mean channel bed slope at Timbuctoo Bend in 2004 was 0.0054.

In May 2005 a flood occurred on the Yuba River caused by a large rainstorm beginning on 15 May, which abated after 2:00 p.m. on 16 May and then resumed again after 6:00 p.m. on 17 May. Rainfall stopped at 5:00 p.m. on 19 May. In the upper Yuba watershed at Lake Spaulding (1572 m above mean sea level), the total rainfall during the event was 218.19 mm, with a peak intensity of 7.87 mm/hr on the evening of 18 May. Prior to the flood, the river was at a base flow of ~ 30 m^3s^{-1} for 6 months with spring snowmelt elevating flows throughout April 2005. The flood peaked at 1215.8 m^3s^{-1} during the night of 21 May 2005. Using log-normal flood frequency analysis on the 1971-2004 dataset, this corresponded to a 7.7 year recurrence interval. By 31 May the flow receded from the floodplain and evidence of channel change warranted investigation. Three weeks later the flow receded to 85 m^3s^{-1}.

3. Methods

A high-resolution, feature-based topographic survey shortly before and shortly after the

May 2005 flood provided key data to characterize channel change at the study site. Digital elevation models (DEMs) from these surveys were used to drive at-a-station hydraulic geometry analysis, 2D hydrodynamic models, and DEM differencing. Hydraulic field data collected before, during, and after the flood were used to prepare and validate the models. Four discharges were analyzed, the autumn low flow (23.4 m^3s^{-1}), present-day Q_b (159.2 m^3s^{-1}), the 1942-1971 Q_b (328.5 m^3s^{-1}), and the peak of the 7.7-year event (1215.8 m^3s^{-1}) that occurred during the 21 May 2005 flood. Together these four discharges represent the low to middle range of the natural flood hydrograph of the Yuba River at Timbuctoo Bend.

3.1. Field Methods

3.1.1. Topography

Topography was mapped in detail before and after the May 2005 flood. For the pre-flood condition, data were collected during the low flow period from September 2004 to March 2005, using methods similar to Brasington et al. (2000), Pasternack et al. (2004, 2006), and Elkins et al. (2007). A Trimble 5700 Real Time Kinematic GPS was used to perform static surveys to establish three permanent benchmarks in geographic coordinates. Corpscon 6.0 was used to convert those coordinates to the projected California State Plane Zone II (NAD83 datum) coordinates and the NAVD88 vertical datum. Working from these benchmarks, a Topcon GTS-802A robotic total station measured bed positions on a staggered grid with supplemental points as needed to resolve bed features (e.g., boulders, slope breaks, redd dunes, etc). The few unwadable locations were mapped by total station using a long prism pole held over the side of a small inflatable raft. After quality checks, the survey yielded 28,008 points with a mean sampling density in the channel of 0.617 points/ m^2. A lower sampling density was used on the relatively flat floodplain, yielding an overall sampling density for the whole study area of 0.418 points/m^2. Surveying accuracy was assessed using 98 control network checks and was found to average 0.013 m in the horizontal and 0.011 m in the vertical, which is significantly smaller than the natural error induced by the bed material, typically ranging in size between 0.05-0.2 m.

For the post-flood condition, site bathymetry was surveyed using a boat-based approach on the falling limb of the flood shortly after bedload transport had abated. The survey was performed on 10-11 June 2005 over which period flows attenuated from 167 to 116 m^3s^{-1}. A private hydrography firm (Environmental Data Solutions, San Rafael, CA) was contracted to partner in this effort to produce a map meeting U.S Army Corps of Engineers' rigorous Class 1 standard (± 0.15m vertical accuracy; USACE, 2002). A customized 6-m long Boston Whaler was outfitted with an Odom Hydrotrack survey-grade fathometer with a 3°, 200-kHz transducer. Geographic positions for the fathometer were collected using a Trimble 5700 real-time kinematic GPS receiving corrections by radio from an on-site base station located on one of the preestablished benchmarks. Both streams of data were integrated in real-time using Hypack Max 4.3 (Hypack, Inc., Middletown, CT). Where depth permitted, the boat made cross sections on ~ 3-m intervals and did six longitudinal transects approximately evenly spaced across the channel. Because bathymetry was mapped during the falling limb of the flood to access as much of the river as possible by boat, it was necessary to account for changes in the water surface slope through time to refine bathymetric mapping. Four Mini Troll 400 vented pressure transducers (In-situ, Inc., Fort Collins, CO) recording water levels once every minute were placed in the river along the study site in suitable hydraulic conditions at key water surface slope breaks and their elevations were surveyed using a total station. An algorithm within Hypack (tide adjustments) was used to interpolate water surface slopes based on the distance between the pressure transducers. In post-processing, a radial filter was applied to the boat-based data to ensure 0.25-m spacing between points. Quality assurance and quality control information beyond the scope of this summary is on file with the contractor. The floodplain was subsequently surveyed with a Leica TPS 1200 robotic total station using the same approach as described above. In September and October 2005 when flow was at its lowest, the Leica total station was used to map all remaining gaps in the data set. In addition, two regions where the boat had been used were resurveyed with the Leica total station as a quality check to compare the results of the two methods. Accounting for both data collection methods and quality checks, a total of 48,914 points were collected to characterize the post-flood surface. The mean sampling density in the channel was 1.14 points/m^2, and for the entire site including the floodplain was 0.73 points/m^2. Topographic data from each survey were imported into Autodesk Land Desktop 3 to create a DEM of the study site pre- and post-flood using a standard TIN-based approach with breaklines (Pasternack et al., 2004, 2006; Wheaton et al., 2004a; Elkins et al., 2007).

3.1.2. Hydraulics

Cross-sectional depth and velocity data were collected along three transects (Fig. 4) on 13 February, 2005 using standard methods appropriate for validating a 2D hydrodynamic model (Pasternack et al. 2004, 2006; Wheaton et al., 2004a; Brown and Pasternack, 2008a). The only modification of the method for this study (on a much wider river) was to use the Topcon GTS-802A to survey the exact position of each paired measurement of depth and velocity, which were collected on average every 2.87-m along a transect. This allowed field data to be precisely compared to model predictions at the same location. Transects 1 and 2 spanned the mainstem channel and were also used to estimate total discharge (Q), whereas transect 3 spanned only the side channel. Measurement errors were ±1 cm for depth using a stadia rod and ±33 mm s^{-1} root mean square for velocity using a Marsh-McBirney Flo-Mate 2000. Velocity was sampled at 30 Hz and averaged over 30 s at 0.6×depth from the water surface to obtain an approximate depth-averaged velocity (Moir and Pasternack, 2008). Studies of flow around individual large grains and pebble clusters demonstrate that point measurements of velocity at arbitrary locations on a gravel-bed will be strongly influenced by these features at the 0.1-0.5 m scale (Paola et al., 1986; Acarlar and Smith, 1987; Kirkbride and Ferguson, 1995; Buffin-Belanger and Roy, 1998; Lawless and Robert, 2001a,b). Thus, one must acknowledge that field observations are inherently noisy across a section, while model simulations lacking subgrid scale details are inherently smooth.

In addition, the water surface elevation (WSE) along the edge of the channel was mapped using the Topcon total station for three of the four discharges modeled in this study (23.4, 328.5, and 1215.8 m^3s^{-1}). Physical indicators of the 1215.8 m^3s^{-1} peak (delineated by bank scour and a line of debris) were surveyed with the Topcon total station the following day during the falling limb.

3.1.3. Sedimentary analysis

Sedimentary characteristics across the entire site were visually assessed and mapped prior to the flood (Moir and Pasternack, 2008). In this procedure, sediment character was defined in terms of the dominant and subdominant size classes (i.e., boulder > 256 mm, cobble 64-256 mm, gravel 2-64 mm, sand and finer < 2 mm, all sizes being intermediate axis diameter). In addition, the “Wolman-walk” procedure (Wolman, 1954) was used to conduct 32 pebble counts at the study site in autumn 2004. Although data were collected at low discharge conditions, flows at certain regions of the site were too deep and/or fast to permit sampling using this technique. Visual assessment of those areas was performed. Thus, samples were not evenly distributed throughout the site or across all morphological units; they tended to be biased toward accessible channel margin locations. At each location, a minimum of 100 particles (mean = 120, range = 100-219) were sampled across a ~ 3 m × 3 m section of the bed. Each sampling location's central point was surveyed using the Topcon total station.

3.2. Scour Pattern Analysis

Whereas many previous studies have evaluated channel hydraulics over a range of discharges to ascertain whether a velocity reversal existed, few have reported the details of topographic change resulting from overbank floods, as recorded using comprehensive digital elevation modeling and DEM differencing. In this study, the pre- and post-flood surveys enabled a comprehensive characterization of flood-induced channel change as well as interpretation of the change in terms of any riffle-pool relief maintenance. Also, the depth and velocity predictions from the 2D model of the flood's peak discharge along with the bed material data enabled prediction of the Shields stress pattern of the river during the flood. A comparison of the Shields stress pattern against the measured topographic changes allows for interpretation of the physical processes occurring during floods.

3.2.1. Channel Change

Pre- and post-flood DEMs were imported into ArcGIS 9.2 where a differencing analysis was performed to characterize the spatial pattern of net scour and deposition from the May 2005 flood at Timbuctoo Bend. The DEM difference (Δz) was calculated by subtracting the 2004 surface from the 2005 surface. Coincident rasters (cell size 0.023 m^2) were generated from triangular irregular network (TIN) elevation models in 3D Analyst and then differenced using Spatial Analyst. The raw differenced surface was then classified to identify areas of scour and deposition. To assess uncertainty in DEM differencing caused by various sources of error, a sensitivity analysis was performed in which different minimum thresholds (0 , ±0.0254 , ±0.0508 , ±0.15 , and ±0.3 m) were set below which the difference values were forced to equal zero. The zonal statistics tool was then used to calculate the gross and net volumetric difference between the DEMs for each threshold value. To convert volumes to masses for this loose gravel and cobble, a density estimate of 1.645 tonnes m^{-3} was used based on the quarry tests of Merz et al. (2006).

The spatial pattern of scour and deposition was inspected to determine whether there was any indication of riffle-pool maintenance. First, the pattern of channel change was evaluated considering the whole domain of the river corridor to determine if there existed foci of change and to qualitatively infer the mechanism responsible for the change. Second, at each cross section, the mean bed elevation of the modern bankful channel was calculated using the pre- and post- flood cross-sectional data sets. Then the change in mean bankful bed elevation from the flood was computed for each cross section and the direction and magnitude of change were used as the key test metrics. Based on the flow convergence routing hypothesis, maintenance would be confirmed by net scour in the upstream pool and net deposition in the riffle. Less corroboration would be provided if the whole channel scoured, as might be expected in a reach lacking sediment supply from upstream. Topographic change in other morphological units was also assessed.

3.2.2. Shields Stress Prediction

Shear velocity (U^*), bed shear stress (τ_b), and nondimensional Shields stress (τ^*) were calculated at each node in the 2D model according to

$$U^* = U / \left(5.75 \log\left(12.2 H / 2 D_{90}\right)\right) \quad (4)$$

$$\tau_b = \rho_w \left(U^*\right)^2 \quad (5)$$

$$\tau^* = \tau_b / \left(\rho_s - \rho_w\right) g D_{50} \quad (6)$$

where U is depth-averaged velocity magnitude at a point, H is water depth, ρ_w is water density, ρ_s is bed particle bulk density, g is gravitational acceleration, and D_{90} and D_{50} are the bed material sizes that 90% and 50% of the bed material is smaller than, respectively (Pasternack et al., 2006). Shields stress values were categorized based on transport regimes defined by Lisle et al. (2000), where values of $\tau^* < 0.01$ correspond to negligible transport, $0.01 < \tau^* < 0.03$ correspond to intermittent entrainment, $0.03 < \tau^* < 0.06$ corresponds to partial transport (Wilcock et al., 1996), and $\tau^* > 0.06$ corresponds to full transport.

To evaluate the role of flood peak hydraulics on channel change, a comparison was made between 2D model τ^* results and DEM difference observations (Δz). Digital elevation model difference values were interpolated to the 2D model's computational mesh nodes where τ^* values had been computed to obtain spatially distributed pairs of $\{\tau^*, \Delta z\}$ at the same location. A scatter plot was made between Δz and τ^* to determine the nature of the relation between the data sets. Also, a box and whisker plot was made to evaluate the distributions of τ^* for erosional (Δz < -0.15 m), no change (Δz within ±0.15 m), and depositional zones (Δz > 0.15 m).

Recognizing that hydraulics and channel change may vary between morphological units, a separate analysis was done isolating the data at the pool, riffle, and run cross sections. Also, to distinguish between in-channel and floodplain dynamics, the cross-sectional data was further subdivided relative to the known bankful elevation. It was hypothesized that τ^* data extracted from the 2D model that exceeded the threshold for partial transport ($\tau^* > 0.03$) should corresponded to observed scour locations. Conversely, locations with low transport capacity (i.e., $\tau^* < 0.03$) should correspond to no change or deposition. This was assessed throughout the whole study site at mesoscale morphological units that play a key role in integrating stream ecology, geomorphology, and hydrology (Moir and Pasternack, 2008).

3.3. At-a-station Analysis

Traditionally, analyses of hydraulics and channel change at cross sections stand as the dominant method for characterizing fluvial geomorphology. This standard method was employed here to promote comparison with historical studies and provide results for those comfortable with the classic approach. WinXSPRO version 3.0, a one-dimensional (1D) resistance equation-based cross section analyzer available through the U.S. Forest Service (Hardy et. al., 2005), was used to obtain at-a-station hydraulic geometry relationships for these cross sections over a wide range of flows. Pool, riffle crest, and run cross sections were extracted from the pre- and post- flood DEMs using Land Desktop 3 for cross section analysis (Fig. 4). WinXSPRO and similar cross-section analyzers assume uniform flow so that bed slope, water surface slope (S_w), and the total energy grade line are parallel at the individual channel cross section location (Hardy et. al., 2005). The program computes hydraulics at increments between specified low and high WSEs. Data inputs for each range of flows investigated included low and high WSE values along with their corresponding Manning's *n* roughness coefficients and S_w values. Outputs included cross-sectional area (m), wetted perimeter (m), width (m), hydraulic depth (m), water surface slope (S_w (m/m)), average velocity from Manning's equation (ms^{-1}), discharge (Q (m^3s^{-1})), and shear stress (Pa). WinXSPRO outputs were then used to calculate width, depth, and velocity at-a-station hydraulic geometry relations for each cross section. Width, depth, velocity, and shear stress were non-dimensionalized using D_{50} (Pitlick and Cress, 2002) to obtain comparable results across a wide range of spatial scales, but are not reported because of similarities between dimensional and nondimensional results.

In order to take advantage of field-measured S_w observations at some stages and optimize the performance of WinXSPRO, each cross section was analyzed incrementally in three sub-sets by Q: (i) 0 to 159.2 m^3s^{-1}, (ii) 159.2 m^3s^{-1} to 328.5 m^3s^{-1}, and (iii) 328.5 m^3s^{-1} to 1,215.8 m^3s^{-1}. The values bounding these ranges relate to observational data and the geomorphically significant discharges described in section 2 above. In each flow range, Manning's n values were selected to match those from the calibrated 2D model simulations described later. First, the WSE at 0 m^3s^{-1} and that estimated for 159.2 m^3s^{-1} were specified along with a constant corresponding Manning's n value of 0.043 for low discharge and 0.042 for high discharge (Moir and Pasternack, 2008). The water surface slope for 159.2 m^3s^{-1} was fixed at 0.0047, but for 0 m^3s^{-1} was adjusted to yield the field-observed water surface slope of 0.0055 at 23.4 m^3s^{-1}. In WinXSPRO, S_w decreases linearly as Q increases. Once the low-Q value of S_w was solved for, the WSE for 159.2 m^3s^{-1} was adjusted to yield a model-estimated discharge as close to 159.2 m^3s^{-1} as possible, while holding the S_w for that WSE constant. For the next Q increment (159.2 to 328.5 m^3s^{-1}), the obtained parameters for 159.2 m^3s^{-1} were used as the low WSE values and the S_w for 328.5 m^3s^{-1} was set to the observed value of 0.003. Manning's n was set at 0.042 and 0.041 for the low and high discharges, respectively. The WSE for 328.5 m^3s^{-1} was adjusted to yield a Q as close to 328.5 m^3s^{-1} as possible. The same approach was repeated again for the highest range of Q, given the observed S_w for 1215.8 m^3s^{-1}. Manning's n was set at 0.041 and 0.039 for the low and high discharges, respectively. In summary, the semi-analytical cross-sectional analyzer WinXSPRO was used to calculate unmeasured hydraulic parameters from observed field data.

3.3.1. WinXSPRO Validation

WinXSPRO assumes steady, uniform flow. Thus, the output data were compared against 2D hydraulics, which better represent nonuniform flow responsible for riffle-pool relief in gravel-bed rivers (MacWilliams et al., 2006). Details of the 2D modeling procedure are presented in the next section. To obtain comparable cross-sectional averages, cross section locations were imported into each 2D model, results were extracted at ~ 2-m intervals, and these values were averaged for each variable. Wetted widths for each cross section were obtained for all discharges. The percent deviation between WinXSPRO and 2D model results was calculated for each variable. Comparisons of both models and field observations were made using hydraulic data though the size of the river and the danger posed by the flood limited the flow range of that data.

3.4. 2D Yuba Model

Two-dimensional (depth-averaged) hydrodynamic models have existed for decades and are used to study a variety of hydrogeomorphic processes (Bates et al., 1992; Leclerc et al., 1995; Miller and Cluer, 1998; Cao et al., 2003). Recently, their use in regulated river rehabilitation emphasizing spawning habitat rehabilitation by gravel placement has been evaluated (Pasternack et al., 2004, 2006; Wheaton et al., 2004a; Elkins et al., 2007). Two-dimensional models have also been applied to better understand the relative benefits of active river rehabilitation versus flow regime modification (Jacobson and Galat, 2006; Brown and Pasternack, 2008a) on regulated rivers. In this study, the long-established 2D model Finite Element Surface Water Modeling System 3.1.5 (FESWMS), implemented within the Surface-water Modelling System (SMS) graphical interface (Environmental Modeling Systems, Inc.), was used to predict hydrodynamics and characterize mean and local velocity reversals at the described cross sections using the preflood topography. FESWMS (or 2D model) solves the vertically integrated conservation of momentum and mass equations to acquire depth-averaged 2D velocity vectors and water depths at each node in a finite element mesh (Froehlich, 1989). A mesh element is "dry" when depth is below a user-defined threshold (set at $1 \times D_{90}$, ~ 0.12 m here); but to the extent possible, the mesh edges were trimmed to closely match the observed wetted area. The 2D model is capable of simulating steady, unsteady, subcritical and supercritical flows. The full equations and other details of the model have been widely reported in the past (Froehlich, 1989; MacWilliams et al., 2006) and need not be reproduced here. Details on the validation procedure used to characterize model uncertainty in this study follow the explanation of model development. 2D models such as FESWMS are not morphodynamic; they cannot explicitly simulate channel changes, such as longitudinal profile adjustments or bed material coarsening. The interesting question is to see just what these models can achieve, as limited as they are.

3.4.1. 2D Model Development

Refined topographic point and breakline data from the pre-flood DEM were imported to SMS for use in the 2D model. A unique computational mesh was developed for each flow investigated and the density of computational nodes was higher relative to the density of the 2004 preflood topographic data used to run the models (Table 1). Each mesh was generated using a built-in paving algorithm without reference to the independently located depth and velocity measurement points. Elevations at nodes were interpolated from DEM elevations using common TIN methods.

To run the 2D model, discharge at the upstream boundary, and water surface elevation at the downstream boundary are necessary model inputs. The base flow discharge was obtained by velocity-area flow gaging, and flood discharges were determined by combining discharges from the U.S. Geological Survey gaging stations on the Yuba River near Smartville (station #11418000) and on Deer Creek (station #11418500), the one significant tributary between Englebright Dam and the study site. The gaging stations are too close together to necessitate accounting for propagation time of the flood wave to the Deer Creek confluence. The water surface elevation at the downstream flow boundary of the study site was measured using the total station described above.

The two primary model parameters in FESWMS include bed roughness as approximated using variable Manning's *n* for a gravel/cobble bed and isotropic kinematic eddy viscosity (*E*). Roughness associated with resolved bedform topography (e.g., rock riffles, boulders, gravel bars, etc.) was explicitly represented in the detailed channel DEM. Two-dimensional model predictions are highly sensitive to DEM inaccuracies (Bates et al., 1997; Hardy et al., 1999; Lane et al., 1999; Horritt et al., 2006), requiring high-resolution topographic mapping as a data collection method. For unresolved roughness, Manning's coefficient (n) was initially estimated as 0.043 for the gravel bed with $D_{50} \sim 60$ mm. Alternately, $n = 0.06$ was estimated for the armoured cobble/boulder bed located in the riffle crest high velocity zone using a standard linear summation method (McCuen, 1989) and 2D modelling studies of similar gravel rivers (Pasternack et al., 2004, 2006). The bed-roughness parameter can vary spatially in a 2D model to account for variable bed sediment facies. However, small (< 0.005) local deviations are expected relative to field-measurement accuracy in gravel-bed rivers comparable to the LYR. The method of Freeman et. al (1998) was used to calculate *n* in fully submerged stands of willows (*Salix exigua*) on the floodplain lining the bankful channel. Manning's *n* in unsubmerged willow stands was set at 0.1. After performing simulations at each discharge with the initial *n* value, Manning's *n* in the bankful channel was calibrated in intervals of 0.001 for each modeled discharge using the available field-measured WSE data (except 159.2 m^3s^{-1} for which there was no WSE data) to obtain the smallest deviation between observed and modeled WSE longitudinal profiles. Two-dimensional models have been reported to be sensitive to large (> 0.01) variations in *n* values (Bates et al., 1998; Lane and Richards, 1998; Nicholas and Mitchell, 2003), and the validation approach described in the next section would reveal that scale of deficiency.

In a study of 2D model sensitivity for a bedrock channel, Miller and Cluer (1998) showed that 2D models are particularly sensitive to the eddy viscosity parameterization used to cope with turbulence. In the model used in this study, eddy viscosity (E) was a variable in the system of model equations, and it was computed using the following standard additional equations developed based on many studies of turbulence in rivers (Fischer et al., 1979; Froehlich, 1989):

$$E = 0.6H \cdot u_* + E_o \tag{1}$$

$$u_* = U\sqrt{C_d} \tag{2}$$

$$C_d = 9.81\frac{n^2}{H^{1/3}} \tag{3}$$

where H is water depth, u_* is shear velocity, U is depth-averaged water velocity, C_d is a drag coefficient, n is Manning's n, and E_0 is a minimized constant (0.033 m^2s^{-1}) necessary for model stability. These equations allow E to vary throughout the channel, which yields more accurate transverse velocity gradients. However, a comparison of 2D and 3D models for a shallow gravel-bed river demonstrated that, even with this spatial variation, rapid lateral variations in velocity are not simulated to the degree that occurs in natural channels, presenting a fundamental limitation of 2D models like FESWMS (MacWilliams et al., 2006).

3.4.2. 2D Model Validation

Two-dimensional models have inherent strengths and weaknesses, thus uncertainty in modelled results needs to be understood and accepted (Van Asselt and Rotmans, 2002). Previous studies using 2D hydrodynamic models for gravel-bed rivers comparable to the lower Yuba River have validated the model for this application and provide valuable information regarding model utility and uncertainty (Pasternack et al., 2004, 2006; Wheaton et al., 2004a; MacWilliams et al., 2006; Elkins et al., 2007; Brown and Pasternack, 2008a). Manning's n was calibrated to minimize the deviation between the observed and predicted longitudinal profile of water surface elevation and final values were in the physically realistic realm. Predicted and observed conditions at independent locations were compared to provide an assessment of model capability and uncertainty.

Three different validation tests were used to evaluate model performance. First, to validate model-calculated eddy viscosity (E), these values were checked against field-based estimates at 23.4 m^3s^{-1} (summer low flow) for the three observational cross sections. Recognizing that E is not a real physical quantity but an artificial model parameter, the difference between field-based estimates and model-calculated values is within the range typically reported for this type of 2D model (MacWilliams et al., 2006; Pasternack et al., 2006).

Second, even though the field-measured WSE longitudinal profiles were used to calibrate Manning's *n* for each simulation, the final deviations between observed and predicted profiles were non-zero. Thus, the deviations between observed and predicted WSE profiles for the final calibrated simulations were used as one metric to characterize the uncertainty in depths and water surface slopes.

Third, recognizing that lateral and longitudinal variation in velocity in a river is highest at low discharge and low during large floods (Clifford and French, 1998), model validation of depth and velocity on the LYR was performed at a low discharge of 23.4 m^3s^{-1} using observed depths and velocities from cross sections 1, 2, and 3 (Fig. 4). Raw statistical metrics were calculated using all data, and comparisons were made on a cross-sectional basis. Two-dimensional models should be viewed as presenting likely outcomes, but with uncertainty. In combination with field-collected empirical data that helps characterize model uncertainty, such models can help researchers obtain a process-based understanding of hydrogeomorphic phenomena.

4. Results

The May 2005 flood caused significant geomorphic change to the study site. Topographic mapping before and after the event characterized the change and revealed that riffle-pool relief increased. According to both models, the locations of highest depth-averaged velocity and τ^* shift multiple times with increasing discharge. To describe the shifts, results from WinXSPRO (cross-section analyzer) and FESWMS (2D hydrodynamic model) will be reported independently and without scrutiny and then the two will be compared. Finally, the Δz results will be related to the τ^* pattern predicted by the 2D model. The exact location in a morphological unit with the local peak velocity and τ^* as predicted by the 2D model does not necessarily occur on the cross section taken for that unit and used for the cross-section analysis. Cross sections were chosen morphologically, not on the basis of the 2D-model hydraulic results. As a result, independent evaluations of peak magnitudes are necessary for the two methods.

4.1. Flood Scour And Deposition

On 21 May 2005, a high flow changed the topography of Timbuctoo Bend. An evaluation was made to determine if these changes yielded "maintenance" (i.e., pool scour and riffle deposition) of the morphological units. The Δz between the 2004 and 2005 surfaces resulted in six locations of major change (Table 3). Starting from upstream, the pool and pool exit (i.e., riffle entrance) units scoured up to ~ 1 m (location 1, Fig. 8). Downstream from that, the horseshoe-shaped, armored crest of the riffle shifted upstream and incised, indicative of knickpoint migration (location 2, Fig. 8). Up to 1.2 m of deposition occurred in the side channel on river right near the riffle migration point (location 4, Fig. 8). Deposition up to 2.3 m occurred downstream from the island/bar complex, mostly along the right side of the main channel (location 5, Fig. 8). Flanking the riffle on either side of the valley, local scour holes adjacent to bedrock outcrops incised 1.8-2.4 m (location 3, Fig. 8). Deposition along the bankful channel margins enhanced the relief of the natural levees already covered with willows prior to the flood. This zone of deposition represented the largest combined area of deposition during the flood (location 6, Fig. 8).

When the flood-induced bed-elevation change within the bankful channel was analyzed on a cross-sectional basis, the pool was the only unit to show net scour. The mean bed elevation changes for the pool, riffle, and run cross sections were -0.35 m (i.e., net scour), 0.07 m (i.e., net deposition), and 0.04 m (i.e., net deposition), respectively. The magnitude of net scour at the pool cross section is a strong signal beyond the level of noise in the DEM differencing analysis, whereas the magnitudes of net deposition in the riffle and run are within the noise and thus can only be regarded as indicative of no net change. Nevertheless, the relief between the riffle and pool cross sections increased by 0.42 m.

4.2. WinXSPRO Results

WinXSPRO analyzed the pool, riffle, and run cross sections and produced at-a-station hydraulic geometry relationships for all discharges 0-1218 m^3s^{-1} (Fig. 5). Five velocity reversals were predicted by WinXSPRO among the three cross sections, as indicated by arrows on Fig. 5C. The key results of the analysis are described below. In this subsection, all hydraulic variables are reported as cross-sectional averages.

4.2.1. Summer Low Flow to Modern Q_b

At discharges below the typical autumn salmon-spawning flow of 23.4 m^3s^{-1}, WinXSPRO predicted that the pool has the lowest velocity and τ^* as well as the widest and shallowest cross section. Conversely, up to 23.4 m^3s^{-1}, the model predicted that the highest velocity and τ^* occurred at the run, where the river was the narrowest and deepest. A velocity reversal occurred at discharges > 23.4 m^3s^{-1}, and at those highest flows pool velocity, depth, and τ^* surpassed those of the riffle but not the run (Fig. 5C; Table 2).

For all discharges between the typical autumn salmon-spawning flow of 23.4 m^3s^{-1} and modern Q_b at 159.2 m^3s^{-1}, the run continued to have the highest predicted velocity and τ^*. As discharge approached modern Q_b, the run became wider. Also, the pool had a higher predicted velocity than the riffle, but at Q_b the velocity and width at the riffle became slightly higher than those at the pool yielding a slight reversal (Fig. 5C). Over a very narrow flow range, the velocity and width at the riffle decreased as discharge increased thereafter, so the pool was restored as the wider and faster cross section after the brief range of riffle ascendancy. These fluctuations are minor responses to differential topography.

4.2.2. Modern Q_b to pre-Bullards Bar Dam Q_b

At discharges greater than present day Q_b, the locations of velocity and τ^* peaks were predicted by WinXSPRO to change, and two velocity reversals were predicted at the cross sections analyzed in this study (Fig. 5). From 159.2 to 328.5 m^3s^{-1}, the width at the run doubled as flow expanded from bankful confinement leading to a slight decrease in average depth. At ~ 200 m^3s^{-1}, the pool velocity and τ^* surpassed those of the run. At these discharges the pool had the deepest cross section. A second reversal was predicted to occur at ~ 300 m^3s^{-1}, at which point the velocity in the run became lower than the riffle. At this flow, the riffle had the widest cross section.

4.2.3. Pre-Bullards Bar Dam Q_b to Peak Flood Flow

At all discharges above 328.5 m^3s^{-1}, the pool cross section was predicted to have the highest velocity magnitude (> 2 m s^{-1}), while the riffle had higher velocities than the run. The pool was deepest and the run shallowest, while the run became the widest cross section for all analyzed discharges above ~ 700 m^3s^{-1}. Shields stress values for the three cross sections showed the same relative magnitudes and trends with increasing discharge as predicted for velocity.

4.3. 2D Model Results

The results of 2D modeling also show velocity reversals in Timbuctoo Bend on the lower Yuba River (Fig. 6; Table 2), but the velocity reversal patterns predicted by the 2D model differ significantly from those predicted by WinXSPRO (Fig. 5, points versus lines). In addition to characterizing shifts in the location of peak velocity on the rising limb of the 1215.8 m^3s^{-1} flood, the 2D model assisted in illustrating the relationship between hydraulics and sediment transport dynamics responsible for maintaining the topography at Timbuctoo Bend.

4.3.1. 2D Model Validation

Measured E values ranged from 0.001 to 0.043 m^2s^{-1}, with a mean of 0.023 m^2s^{-1} (SD = 0.010 m^2s^{-1}). The minimum value of E_0 that could achieve model stability was 0.0355 m^2s^{-1}. Resulting modeled E values were higher than field estimates, ranging from 0.034 to 0.075 m^2s^{-1} with a mean of 0.057 m^2s^{-1} (SD = 0.010 m^2s^{-1}). This shift to higher eddy viscosity values causes greater transference of momentum and more smoothing of velocity gradients across the channel (MacWilliams et al., 2006; Pasternack et al., 2006).

Manning's n values unique to each discharge and surface type were calculated and calibrated, yielding the values reported next. For 23.4 m^3s^{-1}, flow was entirely in the bankful channel and a uniform n of 0.043 was used, except for a value of 0.06 in a small area of armored bed on the riffle crest. At 328.5 m^3s^{-1}, the bankful channel's *n* calibrated to 0.047, left bank floodplain *n* calibrated to 0.045, and willow levee *n* was set at 0.1. For the flood peak discharge of 1215.8 m^3s^{-1}, the bankful channel and floodplain *n* calibrated to 0.039. The Freeman et al (1998) analysis of roughness in fully submerged willow stands yielded an *n* estimate of 0.057.

The final comparison of predicted and observed water surface slopes yielded deviations of < 0.15% error in water surface elevations showing overall good longitudinal predictions. To put these percentages into more meaningful absolute values, in model runs with calibrated Manning's *n* values, mean absolute values of the deviations of predicted WSE at 23.4, 328.5, and 1215.8 m^3s^{-1} were 0.051 m (*SD* = 0.04 m), 0.07 m (*SD* =0.05 m), and 0.10 m (*SD* = 0.09 m), respectively. However, mean raw WSE deviations (observed-modeled) were 0.031 m (*SD* = 0.06), 0.01 m (*SD* = 0.09), and -0.02 m (*SD* = 0.14), respectively for the above discharges. Thus, at the two lower discharges the model slightly under predicted WSE and at the flood flow the model slightly over predicted WSE. The calibration process helped increase model performance and resulted in physically realistic values with acceptable deviations from field-observed water surface elevations.

Hydraulic measurements made at 83 points along three cross sections (Fig. 7) showed moderately accurate model-predicted versus observed depth and velocity values at the low flow of 23.4 m^3s^{-1} (Fig. 7). A coefficient of determination of 0.929 for depth and 0.768 for velocity was observed for predicted versus observed values over all cross sections ($p < 0.001$ for both tests). Average absolute deviation between predicted and observed depth and velocity was 10% and 22%, respectively. One abnormally low velocity measurement at ~ 80 m in cross section 1 (Fig. 7) was excluded from the previous value. Cross section 1 showed that predicted depth and velocity closely matched the observed smoothed best-fit curve. At cross section 2, more lateral variation in depth and velocity occurred, but the general pattern of predicted and observed measurements remained intact. The 2D model under predicted depth and over predicted velocity at cross section 3, but the patterns match. This validation was only performed at low flow because high flow velocity measurements were not feasible or safe. However, as illustrated by the model results, velocity fields at higher flows have less variability at high discharges (Fig. 6).

Model validation for Timbuctoo Bend highlighted the capabilities and limitations of a 2D model for this application as stated by previous studies (Lane et al., 1999; Pasternack et al., 2004, 2006; MacWilliams et al., 2006; Brown and Pasternack, 2008a,b; Moir and Pasternack, 2008). Predicted spatial patterns in depth and velocity can be considered accurate with reasonable confidence, but a 3D model with a more sophisticated turbulence closure algorithm would best capture lateral velocity variations influenced by vertical mass and momentum fluxes. However, the 2D model is practical for this application and valuable if the inherent uncertainties in the simulation process are acknowledged. Future morphodynamic models will go beyond what is possible now.

4.3.2. Model Predictions

The 2D model predicted velocity and τ^* reversals at four discharges, gave results for comparison with WinXSPRO output at each cross section (Fig. 5), and provided a visual representation of the entire modeled reach to better understand spatial results. At summer low flow, the pool was the widest morphological unit and it had the greatest cross-sectional area (Table 2; Fig. 6A). Cross-sectional average velocity at the pool was low (0.36 ms^{-1}, *SD* ±0.10) and τ^* was negligible. The riffle cross section was divided by the mid-channel island (Fig. 6), with the highest velocity flow (mean column 1.12 ms^{-1}, *SD* = 0.58 ms^{-1}) located in the main channel. Shields stress in the riffle at low flow (cross-sectional mean τ*=0.04, *SD* = 0.010) was within the partial transport domain (0.03 < τ* < 0.06). The run cross section was narrow, with moderately high velocity within the channel, but τ^* remained relatively low within the intermittent transport range (0.01 < τ* < 0.03).

At present day Q_b, cross-sectional width and area began to converge at the pool and riffle cross sections (Figs. 5A, 6B). The depth in the pool and riffle also converged at this discharge (Table 2). The velocity in the riffle remained higher than that in the pool because of the funneling effects of the island topography on the shallow flow over this cross section. However, the run cross section concentrated flow through a relatively narrow cross section, so that location had the highest velocity at present day Q_b, yielding a velocity reversal between the riffle and run (Table 2). Even though a velocity reversal was predicted, τ^* was still slightly higher at the exact location of the riffle cross section compared to that of the run (0.048 versus 0.044). However, farther downstream in the run at the model outlet, the velocity and τ^* cross-sectional averages were higher than at the riffle. Both the run and riffle mean τ^* values were within the partial transport domain.

The Pre-Bullards Bar Dam Q_b model results showed that cross-sectional width had mostly equalized between the pool and run units (Fig. 6C; Table 2). However, the width in the run was still narrowest, so the constricted flow induced convective acceleration and yielded the highest velocity there. The zone of highest velocity at the run extended farther upstream compared to the present day Q_b, so the selected cross section location better represented flow conditions in the run at this discharge (Fig. 6C). Velocity remained higher in the run than in the riffle, and τ^* paralleled velocity and was slightly higher in the run than riffle at this discharge – though both were lower than their corresponding values at present day Q_b.

Finally, at the peak flood flow, valley walls constricted flow in the pool, so wetted width was narrowest there and a major velocity reversal occurred. Velocity (mean = 2.33 ms^{-1}, *SD* = 0.081 ms^{-1}), and τ^* (mean = 0.041, *SD* = 0.020) were highest in the pool relative to other cross sections (Table 2). Downstream at the run cross section, the floodplain was less constricted by valley walls, allowing flow to spread out over the adjacent floodplain (Fig. 6D). Compared with the lower discharges, the downstream velocity gradient was significantly lower, while the cross-channel velocity gradient was higher. As assumed in the experimental design for model validation, much less local velocity variation exists at the peak flow compared with that at the lowest flow.

4.4. WinXSPRO versus 2D model

Overall, WinXSPRO overestimated values compared to 2D model predictions of width, depth, velocity, and τ^* (Fig. 5). Given the theoretical assumptions described earlier, WinXSPRO was unable to characterize backwater effects caused by topographic highs. In contrast, the 2D model predicted deeper and slower conditions in the pool at low flows and in the run at high flows as a result of lateral and vertical channel constrictions. At 23.4 m^3s^{-1}, the 2D model predicted depth 50% greater and velocity 149% slower than those predicted by WinXSPRO for the pool cross section. While the riffle exhibited similarity in the predictions of the two methods suggesting approximately uniform flow conditions, the run showed a slight backwater effect with a 4% higher depth and a 23% lower velocity in the 2D model (Fig. 5). At present day Q_b, the 2D model predicted a backwater effect in the pool, with a 28% higher depth and a 58% lower velocity. However, a slight acceleration occurred at the riffle, while the run showed approximately uniform conditions at modern Q_b. Once again, the 2D model predicted velocity

40% lower than WinXSPRO in the pool at 328.5 m^3s^{-1}, indicating the backwater effect of the riffle crest and island width constriction on pool hydraulics. At this discharge, approximately uniform flow conditions existed at the riffle and run units. At 1215.8 m^3s^{-1}, the trend was reversed with the pool showing a slightly higher velocity in the 2D model relative to WinXSPRO. The riffle maintained approximately uniform flow conditions, while the 2D model predicted velocity 15% lower than WinXSPRO in the run at this flow.

An analysis of cross-sectional area, width and depth with increasing discharge can help explain the velocity reversals evident at Timbuctoo Bend. On average WinXSPRO slightly overestimated width by 7% compared to the 2D model. Recognizing that the 2D model turned off near-bank mesh elements where depth was < 0.12 m, this difference is not significant. On average for both methods, the pool was ~ 70% and ~ 130% wider than the riffle and run cross sections at 23.4 m^3s^{-1}, respectively (Table 2). In addition, the pool had the greatest cross-sectional area and the lowest velocity at summer low flow. At present day Q_b, WinXSPRO predicted that mean width, depth, and velocity values in the riffle were similar to those in the pool, but the run had the narrowest cross section. Also, the average velocity in the run peaked at present day Q_b and thus was a function of a low width-to-depth ratio and the smallest relative area of all cross sections (Table 2).

The 2D model deviated from the WinXSPRO estimates because it accounts for channel nonuniformity and the associated flow accelerations and backwater effects. According to the 2D model, the pool had the lowest predicted velocity at 328.5 m^3s^{-1}, while WinXSPRO predicted that the pool and run had approximately the same cross-sectional area and velocity at this discharge (Fig. 5; Table 2). This is consistent with a backwater effect in the 2D model associated with vertical and lateral channel nonuniformity that is absent from WinXSPRO. At

1215.8 m^3s^{-1}, WinXSPRO predicted that the run had the widest cross section with the largest cross-sectional area. Both methods predicted that average velocity was lowest in the run and highest in the pool, though they differed on the exact value (Fig. 5C; Table 2). According to the 2D model, velocity was greater in the pool than predicted by WinXSPRO, because of a smaller cross-sectional area. The pool had the narrowest, deepest cross section at this discharge (Fig. 5) because it was resistant to widening bound by steep bedrock valley walls. The flow was fastest through the pool and then diverged and slowed down exiting the pool. This hydraulic effect was primarily associated with lateral channel nonuniformity.

Shields stress predictions also varied between the two models, corresponding to the differences in velocity described above. For example, at summer low flow, WinXSPRO overestimated velocity at the pool cross section because of the inability to predict backwater effects. Shields stress at the pool exit was 0.020 as predicted by WinXSPRO and close to 0.000 (±0.001) for the 2D model (Table 2). The same occurred at the run, but WinXSPRO underestimated τ^* on the riffle (0.026 compared to 0.040, *SD* = 0.010) at low flow. Shields stress deviations between the two methods correspond to the difference between velocity predictions for all cross sections (Table 2). Notably, τ^* was predicted to be the highest at the pool at peak flood flow by both methods (Table 2; Fig. 5)

4.5. Accuracy of Sediment Transport Regime Predictions

A key objective of this study was to test the predictive ability of the 2D model to characterize sediment transport capacity related to observed net scour and deposition patterns. A regression analysis of raw Δz versus predicted τ^* at the flood's peak Q (n = 1001) yielded a coefficient of determination (r^2) value of 0.03. When model-predicted τ^* data for the flood peak were stratified by direction of channel change (i.e., scour, no change, or deposition), then significant differences were apparent (Fig. 9). Areas of no significant change had the lowest values for the 25th, 50th, 75th, and 90th percentiles of τ^*, while areas of significant scour had the highest of all of those values. Areas of deposition had higher τ^* at the flood peak than those with no significant topographic change.

Unlike the bulk analysis between raw τ^* and Δz, when stratified by morphological unit (i.e., the pool, riffle, and run cross sections), scour and deposition showed a strong systemic response to model-predicted τ^* at the flood peak (Fig. 10). The observed pattern can be explained based on the underlying mechanisms captured by the 2D model. Where the 2D model predicted $\tau^* > 0.045$, scour dominated (Fig. 10). Where the model predicted $\tau^* < 0.03$, deposition dominated. In between those thresholds is the domain of partial transport in which both deposition or scour are possible, but in very small net amounts overall. The one exception being that within the willows bordering the channel significant deposition took place during partial transport because of the ability of the dense plant thicket to capture sediment (Fig. 10).

The majority of the pool cross section was characterized by 0.15-0.5 m of scour and $\tau^* >$ 0.045 (Figs. 10A, 11A). The location of deepest scour (~ 1 m) along the left bank of the bankful channel corresponded with a τ^* of 0.049 and decreased toward the bank. Some bank scour was associated with intermediate τ^*, possibly facilitated by smaller particle sizes and bank undercutting. In addition, deposition occurred on the vegetated floodplain adjacent to the pool's left cutbank in shallower areas (~ 2-3 m deep) with moderately low velocity (~ 1.5 m s^{-1}) and τ^* (0.01-0.02) (Figs. 10A, 11A). Together these factors increased bank steepness and sharpened the delineation between channel and floodplain (Figs. 8, 11). Equivalent bank scour did not occur on river right since the bank there was composed of bedrock.

At the riffle cross section three distinct zones of matching bed change and τ^* existed (Figs. 10B, 11B). Knickpoint migration of the horseshoe riffle crest scoured 0.15-1 m down through the riffle, in which location the model-predicted τ^* was between 0.046-0.052. Over the island and side channel (evident below contemporary bankful discharge), deposition occurred where τ^* was between 0.02-0.034. The rest of the cross section showed no significant change in bed elevation and had intermediate τ^* values of 0.034-0.045. Relative to the other two cross sections, the floodplain adjacent to the riffle experienced no significant elevation change.

The run cross section was predominantly depositional, because of a wide, deep cross section and corresponding low mean cross-sectional velocity during the flood peak. The mean velocity including the delineated floodplain was the lowest at the run as predicted by both modeling methods (Table 3), with an active mid-channel zone of relative highest velocity (Fig. 6D) and a local τ^* maximum of 0.04 (Fig. 11C) mid-channel. This cross section experienced 0.15-0.8 m of deposition, with the majority occurring along both vegetated banks (Fig. 11C) where τ^* was 0.02-0.04. On the floodplain adjacent to the run, deposition occurred over the vegetated levees where Shields stresses were ~ 0.04 (Figs. 8, 11). At these locations, floodplain deposition occurred in relatively deep (up to ~ 4 m) and fast (up to ~ 2.5 m^3s^{-1}) water (Fig. 10). Some scour also occurred on the floodplain south of the willow levee on river left (Fig. 8), possibly caused by flow rerouting around vegetation. In summary, DEM differencing results demonstrate a threshold-like differentiation of Shields stress values between areas dominated by scour versus deposition when data are stratified by morphological unit.

5. Discussion

5.1. Riffle-Pool Maintenance

An overbank flood with a 7.7-year recurrence interval occurred on the regulated, gravel-bed lower Yuba River causing geomorphically significant changes. High-resolution DEMs and DEM differencing found that the upstream pool scoured, the riffle scoured and aggraded in different subunits (e.g., knickpoint, exposed bar, and side channel features), the run aggraded, and the floodplain aggraded. Cross section analysis confirmed that the net channel change caused by the flood accentuated pool-riffle relief by 0.42 m. That outcome is consistent with the definition of "maintenance" of riffle and pool morphology; meaning that over time riffles remain topographically high and pools remain topographically low. Thus, the presence of maintenance is confirmed at the study site for this one flood event.

A limitation of this study is that it focuses on evaluating the mechanisms of channel maintenance during a single flood and does not evaluate interdecadal persistence of the riffle-pool unit or what would promote that for decades and beyond. Further, the mechanisms observed could be specific to unique local conditions that might not exist at other riffle-pool units. To gain insight into the broader geomorphic context, aerial photos of the reach that this site is located in spanning 1937-2008 were studied by White (2008). He confirmed that over several decades a pool-riffle unit existed at the study site. The exact morphology and longitudinal position of the riffle have changed within a narrow limit over decades, but the pool remains a pool and the riffle remains a riffle. White (2008) used geomorphic analyses of aerial photos and topographic maps of the whole Timbuctoo Bend river corridor to show that persistent pools are located in valley width constrictions and persistent riffles in valley width expansions. Figure 3 illustrates the persistence of fluvial forms, including riffle-pool units in Timbuctoo Bend over ~100 years, despite flow regulation. This observational evidence is consistent with expected dynamics associated with flow convergence routing over a much wider range of flows than investigated in this study of a single site. Consequently, both detailed quantitative metrics over a single flood event and photo-based analysis spanning decades agree that the study site exhibits riffle-pool maintenance and that other riffle-pool units with diverse morphologies in the same reach also exhibit riffle-pool maintenance.

5.2. Spatially Variable Sediment Competence

It is commonly perceived that during low flows little to no sediment transport occurs in a gravel-bed river and thus no significant channel change occurs. Further, a common postulation reads that a minimum threshold exists, commonly defined as $\tau^* = 0.03$ or 0.045, above which "partial transport" occurs (Wilcock et al., 1996). When $\tau^* > 0.06$, a sheet of sediment is in transport with a thickness of 1-2 times D_{90} (Lisle et al., 2000). Thus, the primary scientific goals in evaluating sediment transport and channel change are to determine (i) the Q at which sediment transport begins, (ii) the "effective discharge" at which annualized sediment transport is maximized in combinations with frequency distribution of the flow regime, and (iii) the Q that is responsible for controlling channel morphology on the decadal timescale (Andrews and Nankervis, 1995). The new results from this study raise concerns about this conceptual framework.

Previous studies have questioned the existence and measurability of a minimum threshold in τ^* before sediment transport begins. Paintal (1971) performed long-duration sediment-transport flume experiments and found that "…a distinct condition for the beginning of movement does not exist" and that defining such an arbitrary threshold is of "no practical importance." Wilcock (1988) described the conundrum of significantly different threshold values being obtained by different measurement methods. Using special bedload traps in gravel-bed rivers, Bunte and Abt (2005) found a similar result as Paintal (1971) did in the flume in that observed bedload transport rates were different depending on the duration of observation. Finally, stable morphological units with simple cross sections and simple morphological controls yielding a simple, one-to-one functional relation between Q and τ^* are commonly investigated in bedload transport flume and field studies. The relevance of such simplicity to naturally complex channels is highly debatable.

This study contributes an important new finding; in fact large gravel-bed rivers have significant channel nonuniformity at multiple spatial scales, and consequently exhibit spatially variable sediment transport competence as a function of discharge (Fig. 6). Velocity and τ^* at any point in a river generally increase as a function of discharge as long as the same morphologic control governs hydraulics, as assumed by many sediment-transport studies. However, when the morphologic control at a site shifts from a smaller scale feature of channel nonuniformity to a larger scale one, such as from riffle-pool elevation undulation to valley width undulation, then the shape of the Q versus τ^* function changes and τ^* can decrease or stay the same, as exhibited by the lines and points in Figure 5D. The stronger the channel nonuniformity and the more scales over which it changes, the more spatially and temporally variable the sediment transport function will become. Thompson et al. (1996, 1998) recognized the effects of higher local velocity at a pool head from channel constriction. Also, Cao et al. (2003) noted that constricted channel conditions could lead to competence reversal in some cases depending on combinations of channel geometry, flow discharge, and sediment properties. In this study, the single highest local velocity and τ^* on the riffle was predicted by the 2D model to occur at the lowest discharge (Fig. 6). Thus, bedload transport rate and the greatest potential for localized riffle change should occur at a low discharge when channel nonuniformity causes the riffle to act as a weir (Harvey et al., 1993; Clifford and French, 1998; Brown and Pasternack, 2008a) and exhibits transcritical or supercritical hydraulic conditions. When integrated over the long duration of low flow common to most rivers, this process of riffle scour is enhanced. Even though the sediment eroded off riffles will not transport far, given low τ^* in downstream morphological units during low flow, we have observed on several gravel-bed rivers in the western United States that local channel change is highly ecologically significant, because it creates diverse sedimentary deposits with local hydraulic complexity that can serve many species' needs at different lifestages (e.g. Wheaton et al., 2004b; Pasternack, 2008). In contrast to riffles, this study finds that pools tend to show the expected function of increasing τ^* with increasing discharge (Figs. 5, 6).

5.3. Velocity and Shields Stress Reversals

The results of this study are consistent with past studies reporting reversals in maximum hydraulic parameters from riffles at low flow to pools at high flow (Keller, 1971; Lisle, 1979; Booker et al., 2001). Despite inherent model uncertainties, the field-validated computational methods used in this study described a reversal in section-averaged velocity and nondimensional bed shear stress from riffle to pool with increasing discharge. Further, where the 2D model predicted $\tau^* > 0.045$, the measurable channel change was primarily net scour. Conversely, where τ^* was < 0.03, the channel change was primarily net deposition. Although there was not a simple, continuous function defining the τ^* versus scour depth relation, the directionality of model predictions and observations did match, providing strong evidence of the validity and utility of the 2D model to predict the direction of channel change within a particular channel unit.

Clifford and Richards (1992) stated that sediment competence reversal occurs at 50-90% Q_b based on cross section studies at relatively low discharge in the River Quarme, UK, a small lowland stream channel. In the present study, a double competence reversal occurred in a contiguous riffle-pool sequence in a much larger river channel, with those reversals occurring at $Q \geq Q_b$. First, velocity and τ^* (a surrogate for sediment transport competence) were highest in the riffle for discharges up to Q_b, at which point there are velocity and τ^* reversals. Under this low-flow regime, bankful channel morphology and a large island created the nonuniformity that controlled hydraulic convective acceleration. Second, from 1-2$\cdot Q_b$ the run had highest relative competence. In this flow range, willow-influenced natural levees and the wide floodplain served as hydraulic controls constricting the run much more so than the riffle or pool. Finally, at the highest discharge analyzed in this study (7.63$\cdot Q_b$), the pool had highest relative competence, indicating that a second reversal occurred between those two modeled flows. Pool dimensions during the flood peak were constrained by the valley walls. This overall linked morphologic-hydraulic behavior can be described as a series of "transient reversals" (Clifford and Richards, 1992) with competence reversals occurring dependent on the expression of different scales of channel constrictions and expansions at different discharges. Contrary to Lisle and Hilton (1992), sediment transport competence depends on depth where deposition occurs in the shallowest cross section (run). However, mean cross-sectional depth and width are inversely related at high flows as a function of valley wall constrictions at each cross section. At discharges where the pool was the deepest and narrowest cross section, the greatest magnitude of scour was observed. In a 3D modeling experiment, Booker et al. (2001) concluded that near-bed flow direction routes sediment away from the deepest part of pools; therefore, riffle-pool morphology is maintained by a lack of sediment input into pools rather than increased erosion within pools from convergent flow. The results from this study, though based on a 2D model, indicate that erosion occurred in the deepest part of the pool because of convergent flow at a constricted location and that deposition occurred alongside the active transport zones in the riffle and run downstream. However, these results may have differed if the pool exhibited greater lateral variability adjacent to a large gravel bar. Thus, the hypothesis of "flow convergence routing" (MacWilliams et al., 2006) in conjunction with low-intermediate maintenance flows and persistent bank vegetation describes mechanisms responsible for riffle-pool morphology maintenance at the study site on the LYR.

River restoration practitioners may find a better understanding of channel maintenance mechanisms useful for effective design. One approach to limiting channel scour that is used in river restoration design is to undersize a channel to diffuse flows out onto the floodplain. When this approach is applied with the belief that it will limit peak depth and thus implicitly limit bed shear stress (assuming steady, uniform flow) and channel scour, there is significant risk that the underlying design concept will fail. To the extent that floodplain routing may abate flow constriction with rising discharge, it could reduce channel scour, but that would have to be checked on a site-by-site basis with a 2D or 3D model. Similarly, we have observed and photographed situations in which newly created or rehabilitated pools were excavated from the side to meet a depth specification, but in which the common practice of using an excavator led to an overwidening of ~20-30% beyond the designed width. In such cases, no alarm was raised, because width was not perceived to be a control on channel scour. However, flow divergence in such overwidened pools promotes infilling and a loss of riffle-pool relief. This is often perceived as "natural adjustment" showing the river is behaving naturally, when in fact it is a demonstration of the violation of the underlying assumptions of a restoration's design concept.

In summary, this study supports that limiting depth in channel design is not adequate to achieve control over channel maintenance mechanisms.

5.4. Hydraulic Geometry Limitations

WinXSPRO, a standard cross section analyzer for hydraulic geometry, is commonly used in practice to evaluate and design river channels and geomorphic features. It is a very different tool from a 1D hydraulic model (e.g. HEC-RAS or MIKE11) in that it is only accurate when channels are "approximately" uniform. How does one know if a channel is in fact "approximately" uniform for any given reach? By definition, riffles and pools in gravel-bed rivers are significant topographic highs and lows, respectively. Over a wide range of discharges, riffle crests impose a backwater effect on upstream morphological units and a nonuniform flow acceleration over and downstream from themselves (Pasternack et al., 2008). Therefore, a 1D semi-analytical equation should not be expected to accurately predict hydraulics in riffle-pool sequences. A channel can become submerged to a depth at which vertical bed variability becomes an insignificant fraction of total depth, but under that condition lateral variability in channel and valley widths may impose significant channel nonuniformity, still violating the key assumption of WinXSPRO (Pasternack, 2008). For example, in this study we found that the domain of poor performance of WinXSPRO in predicting velocity and τ^* ranged from 0-7.6$\cdot Q_b$. Over that domain, the tool predicted five velocity reversals, but the validity of that assessment is questionable. Brown and Pasternack (2008b) performed thorough comparisons of hydraulic geometry methods similar to WinXSPRO, 1D numerical modeling (HEC-RAS), and 2D modeling (FESWMS) at predicting hydraulics for two different configurations of pool-riffle-pool sequences lacking velocity reversals. They found that even under that simpler condition, hydraulic geometry methods performed poorly. Both MacWillians et al., (2006) and Brown and Pasternack (2008b) reported that 1D hydraulic models (e.g. HEC-RAS) did not capture important hydraulic mechanisms that are needed to reasonably predict geomorphic processes and ecological conditions.

5.5. 2D Model Limitations

Two-dimensional models account for channel nonuniformity associated with morphological units and predict local depth to within ~ 10% and local depth-averaged velocity to within ~ 25%. However, because many 2D models use a constant eddy viscosity to address turbulence closure, they underestimate the lateral variability in velocity magnitude relative to 3D models (MacWilliams et al., 2006). Also, near-bed velocity and complex 3D flow fields that a 2D depth-averaged velocity model cannot capture cause bed scour (Keller, 1969, 1971; Clifford and Richards, 1992; MacWilliams et. al., 2006). Although near-bed velocity is a good approximation of local sediment transport competence (Rubey, 1938; Keller, 1971; Clifford and Richards, 1992), field collection of such data is not feasible at high flows mobilizing the bed. Two-dimensional models tend to overestimate τ^* (Lane et al., 1999), though two studies (one modeling study and one empirical study) have shown that the overestimation can be corrected for by dividing predicted values by two (MacWilliams et al., 2006; Pasternack et al., 2006). Further, 2D models are not morphodynamic, so they are unable to adjust their boundary in response to scour/ deposition. Thus, to the extent that complete mechanisms explaining riffle-pool maintenance depend on dynamic changes to channel form and surface roughness, 2D models will never achieve a fully satisfying predictive capability.

6. Conclusion

A study combining field measurements, cross section analysis, and mechanistic numerical modeling has revealed that a large gravel-bed river exhibited maintenance of a riffle-pool unit during a flood with a 7.7-year recurrence interval and a peak magnitude of $7.63 \cdot Q_b$. Comparing the topography before and after the flood, riffle-pool relief increased 0.42 m. Further, multiple scales of channel nonuniformity and a dynamic flow regime were found to be ultimately responsible for the observed maintenance because they drive the mechanism termed "flow convergence routing" by MacWilliams et al., (2006). Spatially complex patterns of scour and deposition at the scale of subwidth morphological units were reasonably predicted by the 2D mechanistic model that accounts for convective acceleration, whereas the cross section based method underperformed the 2D model considerably. The 2D model failed to accurately predict the magnitude of point-scale channel change, likely because that is governed by highly localized bed material properties, subgrid scale gravel-cobble structures, and bank vegetation dynamics. Flow convergence routing and the ability of 2D models to capture it will be useful to guide more process-based river restoration projects (e.g., Elkins et al., 2007).

Acknowledgements

Financial support for this work was provided by the U.S. Fish and Wildlife Service Anadromous Fish Restoration Program (Agreement #113323J011). The authors gratefully acknowledge Carlos Alvarado, Blake Andrews, Mary Berta, Mike Bezemek, Evan Buckland, Eve Elkins, Marisa Escobar, Kari Fish, Aaron Fulton, Dave Van Herrick, Lauren Hilliard, Ryan Keating, Donald Moir, Scott Morford, Cameron Poya, Carrie Simms, Nakul Thomas, Ben

Torchia, Julie Tuck, Conner Voss, and Jason White for their assistance in collection of field data and performing data analyses.

References

Acarlar, M.S., Smith, C.R., 1987. A study of hairpin vortices in a laminar boundary layer: Part 1. Hairpin vortices generated by a hemispherical protuberance. Journal of Fluid Mechanics 175, 1-41.

Andrews, E.D., Nankervis, J.M., 1995. Effective discharge and the design of channel maintenance flows for gravel-bed rivers. In: Costa, J.E., Miller, A.J., Potter, K.W., Wilcock, P.R. (Eds.), Natural and Anthropogenic Influences in Fluvial Goemorphology. Geophysical Monograph 89, American Geophysical Union, Washington, DC, pp. 151-164.

Bates, P.D., Anderson, M.G., Baird, L., Walling, D.E., Simm, D., 1992. Modelling floodplain flow with a two dimensional finite element scheme. Earth Surface Processes and Landforms 17, 575-588.

Bates, P.D., Anderson, M.G., Hervouet, J.M., Hawkes, J.C., 1997. Investigating the behaviour of two-dimensional finite element models of compound channel flow. Earth Surface Processes and Landforms 22 (1), 3-17.

Bates, P.D., Horritt, M.S., Hervouet J.M., 1998. Investigating two-dimensional, finite element predictions of floodplain inundation using fractal generated topography. Hydrological Processes 12 (8), 1257-1277.

Booker, D.J., Sear, D.A., Payne, A.J., 2001. Modelling three-dimensional flow structures and patterns of boundary shear stress in a natural pool-riffle sequence. Earth Surface Processes and Landforms 26, 553-576.

Brasington, J., Rumsby, B.T., McVey, R.A., 2000. Monitoring and modelling morphological change in a braided gravel-bed river using high resolution GPS-based survey. Earth Surface Processes and Landforms 25, 973-990.

Brown, A.V., Brown, K.B., 1984. Distribution of insects within riffles of streams. Freshwater Invertebrate Biology 3, 2-11.

Brown, R.A., Pasternack, G.B., 2008a. Engineered channel controls limiting spawning habitat rehabilitation success on regulated gravel-bed rivers. Geomorphology 97, 631-654.

Brown, R.A., Pasternack, G.B., 2008b. Comparison of methods for analyzing salmon habitat rehabilitation designs for regulated rivers. River Research and Applications, 25, 745-772, doi: 10.1002/rra.1189.

Buffin-Belanger, T., Roy, A.G., 1998. Effects of a pebble cluster on the turbulent structure of a depth-limited flow in a gravel-bed river. Geomorphology 25, 249-267.

Bunte, K., Abt, S.R., 2005. Effect of sampling time on measured gravel bed load transport rates in a coarse-bedded stream. Water Resources Research 41:W11405, doi:10.1029/2004WR003880.

Cao, Z., Carling, P., Oakey, R., 2003. Flow reversal over a natural riffle-pool sequence: a computational study. Earth Surface Processes and Landforms 28, 689-705.

Carling, P.A., 1991. An appraisal of the velocity reversal hypothesis for stable riffle-pool sequences in the River Severn, England. Earth Surface Processes and Landforms 16, 19-31.

Clifford, N.J., French, J.R., 1998. Restoration of channel physical environment in smaller, moderate gradient rivers: geomorphological bases for design criteria. In: Bailey, R.G., Jose, P.V., Sherwood, B.R. (Eds.), United Kingdom Floodplains. Westbury Academic & Scientific Publishing, Otley, UK, pp. 63-82.

Clifford N.J., Richards, K.S., 1992. The reversal hypothesis and the maintenance of riffle-pool sequences: a review and field appraisal. In: Carling, P.A., Petts, G.E. (Eds.), Lowland Floodplain Rivers: Geomorphological Perspectives. John Wiley and Sons Ltd., Chichester, UK, pp. 43-70.

Curtis, J.A., Flint, L.E., Alpers, C.N., Yarnell, S.M., 2005. Conceptual model of sediment processes in the upper Yuba River watershed, Sierra Nevada, CA. Geomorphology 68, 149-166.

Elkins, E.E., Pasternack, G.B., Merz, J.E., 2007. The use of slope creation for rehabilitating incised, regulated, gravel-bed rivers. Water Resources Research 43, W05432, doi:10.1029/2006WR005159.

Fischer, H.B., List, E.J., Koh, R.C.Y., Imberger, J., Brooks, N.H., 1979. Mixing in Inland and Coastal Waters. Academic Press, Inc., New York.

Froehlich, D.C., 1989. Finite Element Surface-water Modeling System: Two-dimensional Flow in a Horizontal Plane User's Manual. Publication #FHWA-RD-88-177, U.S. Department of Transportation, Washington, DC.

Freeman, G.E., Copeland, R.R., Rahmeyer, W.J., 1998. Field determination of Manning's n value for shrubs and woody vegetation. United States Committee on Irrigation and Drainage Conference on Shared Rivers, October 28-31, Park City, UT.

Gilbert, G.K., 1914. The Transportation of Debris by Running Water. Professional Paper, Vol. 86. U.S. Geological Survey, Washington, DC.

Gilbert, G.K., 1917. Hydraulic-mining Debris in the Sierra Nevada. Professional Paper, Vol. 105. U.S. Geological Survey, Washington, DC.

Giller, S., Malmqvist, B., 1998. The Biology of Streams and Rivers. Oxford University Press, Oxford, UK.

Gorman, O.T., Karr, J.R., 1978. Habitat structure and stream fish communities. Ecology 59 (3), 507-515.

Hardy, R.J., Bates, P.D., Anderson, M.G., 1999. The importance of spatial resolution in hydraulic models for floodplain environments. Journal of Hydrology 216 (1-2), 124-136.

Hardy, T., Panja, P., Mathias, D., 2005. WinXSPRO, A Channel Cross Section Analyzer, User's Manual, Version 3.0. General Technical Report RMRS-GTR-147, U.S. Department of Agriculture, Forest Service, Rocky Mountain Research Station, Fort Collins, CO.

Harvey, M.D., Mussetter, R.A., Wick, E.J., 1993. A physical process-biological response model for spawning habitat formation for the endangered Colorado squawfish. Rivers, 4 (2), 114-131.

Horritt, M.S., Bates, P.D., Mattinson, M.J., 2006. Effects of mesh resolution and topographic representation in 2D finite volume models of shallow water fluvial flow. Journal of Hydrology 329 (1-2), 306-314.

Jacobson, R.B., Galat, D.L., 2006. Flow and form in rehabilitation of large-river ecosystems – an example from the lower Missouri River. Geomorphology 77, 249-269.

James, L.A., 2005. Sediment from hydraulic mining detained by Englebright and small dams in the Yuba basin. Geomorphology 71, 202-226.

Keller, E.A., 1969. Form and fluvial processes of Dry Creek, near Winters California, M.S. Thesis, Department of Geology, University of California, Davis.

Keller, E.A., 1971. Areal sorting of bed-load material: the hypothesis of velocity reversal.

Geological Society of America Bulletin 82, 753-756.

Keller, E.A., Florsheim, J.L., 1993. Velocity reversal hypothesis: a model approach. Earth Surface Processes and Landforms 18, 733-740.

Kirkbride, A.D., Ferguson, R.I., 1995. Turbulent flow structure in a gravel-bed river: Markov chain analysis of the fluctuating velocity profile. Earth Surfaces Processes and Landforms 20, 721-733.

Kondolf, G.M., 1997. Hungry water: effects of dams and gravel mining on river channels. Environmental Management 21 (4), 533-551.

Lane, E.W., Borland, W.M., 1954. River-bed scour during floods. American Society of Civil Engineers Transactions 119, 1069-1080.

Lane, S.N., Bradbrook, K.F., Richards, K.S., Biron, P.A., Roy, A.G., 1999. The application of computational fluid dynamics to natural river channels: three-dimensional versus two-dimensional approaches. Geomorphology 29 (1-2), 1-20.

Lane, S.N., Richards, K.S., 1998. High resolution, two-dimensional spatial modelling of flow processes in a multi-thread channel. Hydrological Processes 12 (8), 1279-1298.

Lawless, M., Robert, A., 2001a. Scales of boundary resistance in coarse-grained channels: turbulent velocity profiles and implications. Geomorphology 39, 221-238.

Lawless, M., Robert, A., 2001b. Three-dimensional flow structure around small-scale bedforms in a simulated gravel-bed environment. Earth Surface Processes and Landforms 26, 507-522.

Leclerc M., Boudreault, A., Bechara, J.A., Corfa, G., 1995. Two-dimensional hydrodynamic modeling: a neglected tool in the instream flow incremental methodology. Transactions of the American Fisheries Society 124, 645-662.

Lisle, T.E., 1979. A sorting mechanism for a riffle-pool sequence. Geological Society of America Bulletin 90 (11), 1142-1157.

Lisle, T.E., 1986. Stabilization of a gravel channel by large streamside obstructions and bedrock bends, Jacoby Creek, northwestern California. Geological Society of America Bulletin 97, 999-1011.

Lisle, T.E., Hilton, S., 1992. The volume of fine sediment in pools: an index of sediment supply in gravel-bed streams. Water Resources Bulletin 28, 371-383.

Lisle, T.E., Nelson, J.M., Pitlick, J., Madej, M.A., Barkett, B.L., 2000. Variability of bed mobility in natural, gravel-bed channels and adjustments to sediment load at local and reach scales. Water Resources Research 36 (12), 3743-3755.

Lower Yuba River Fisheries Technical Working Group (LYRFTWG), 2005. Draft Implementation Plan for Lower Yuba River Anadromous Fish Habitat Restoration: Multi-agency Plan to Direct Near-term Implementation of Prioritized Restoration and Enhancement Actions and Studies to Achieve Long-term Ecosystem and Watershed Management Goals. Lower Yuba River Fisheries Technical Working Group, Sacramento, CA.

MacWilliams, M.L., Wheaton, J.M., Pasternack, G.B., Kitanidis, P.K., Street, R.L., 2006. The flow convergence-routing hypothesis for riffle-pool maintenance in alluvial rivers. Water Resources Research 42, W10427, doi:10.1029/2005WR004391.

McCuen, R.H., 1989. Hydrologic Analysis and Design. Prentice Hall, Englewood Cliffs, NJ.

Merz, J.E., Pasternack, G.B., Wheaton, J.M., 2006. Sediment budget for salmonid spawning habitat rehabilitation in the Mokelumne River. Geomorphology 76 (1-2), 207-228.

Miller, A.J., Cluer, B.L., 1998. Modeling considerations for simulation of flow in bedrock channels. In: Wohl, E.E., Tinkler, K.J. (Eds.), Rivers Over Rock: Fluvial Processes in Bedrock Channels. Geophysical Monograph Series, Vol. 107., American Geophysical Union, Washington, DC, pp. 61-104.

Moir, H. J., Pasternack, G.B., 2008. Interactions between meso-scale morphological units, stream hydraulics and chinook salmon (*Oncorhynchus tshawytscha*) spawning habitat on the Lower Yuba River, California. Geomorphology 100, 527-548.

Montgomery, D.R., Buffington, J.M., 1997. Channel reach morphology in mountain drainage basins. Geological Society of America Bulletin 109 (5), 596-611.

Nicholas, A.P., Mitchell, C.A., 2003. Numerical simulation of overbank processes in topographically complex floodplain environments. Hydrological Processes 17, 727-746.

O'Neill, M.P., Abrahams, A.D., 1984. Objective identification of pools and riffles. Water Resources Research 20, 921-926.

Paintal, A.S., 1971. Concept of critical shear stress in loose boundary open channels. Journal of Hydraulic Research 9 (1), 91-113.

Palmer, M.A., Ambrose, R.F., Poff, N.L., 1997. Ecological theory and community restoration ecology. Restoration Ecology 5, 291-300.

Paola, C., Gust, G., Southard, J.B., 1986. Skin friction behind isolated hemispheres and the formation of obstacle marks. Sedimentology 33, 279-293.

Pasternack, G.B., 2008. SHIRA-Based River analysis and field-based manipulative sediment transport experiments to balance habitat and geomorphic goals on the lower Yuba River., University of California at Davis, Davis, CA.

Pasternack, G.B., Bounrisavong, M.K., Parikh, K.K., 2008. Backwater control on riffle-pool hydraulics, fish habitat quality, and sediment transport regime in gravel-bed rivers. Journal of Hydrology 357 (1-2), 125-139.

Pasternack, G.B., Wang, C.L., Merz, J., 2004. Application of a 2D hydrodynamic model to reach-scale spawning gravel replenishment on the lower Mokelumne River, California. River Research and Applications 20 (2), 205-225.

Pasternack, G.B., Gilbert, A.T., Wheaton, J.M., Buckland, E.M., 2006. Error propagation for velocity and shear stress prediction using 2D models for environmental management. Journal of Hydrology 328, 227-241.

Pitlick, J., Cress, R., 2002. Downstream changes in the channel geometry of a large gravel bed river. Water Resources Research, 38 (10), 1216, doi:10.1029/2001WR000898.

Richards, K.S., 1976a. Channel width and the riffle-pool sequence. Geological Society of America Bulletin 87, 883-890.

Richards, K.S., 1976b. The morphology of riffle-pool sequences. Earth Surface Processes and Landforms 1, 71-88.

Rubey, W.W., 1938. The Force Required to Move Particles in a Stream Bed. Professional Paper Vol. 189-E, US Geological Survey, Washington, DC, pp. 121-141.

Teleki, P.G., 1971. Areal sorting of bed load material: the hypothesis of velocity-reversal: discussion. Geological Society of America Bulletin 83, 911-914.

Thompson, D.M., Wohl, E.E., Jarrett, R.D., 1996. A revised velocity reversal and sediment-sorting model for a high-gradient, pool-riffle stream. Physical Geography 17, 142-156.

Thompson, D.M., Nelson, J.M., Wohl, E.E., 1998. Interactions between pool geometry and hydraulics. Water Resources Research 34 (12), 3673-3681.

Thompson, D.M., Wohl, E.E. and Jarrett, R.D., 1999. Velocity reversals and sediment sorting in pools and riffles controlled by channel constrictions. Geomorphology, 27(3-4): 229-241.

U.S. Army Corps of Engineers. 2002. Hydrographic Survey Manual. Engineering and Design Manual No. EM-1110-2-1003, U.S. Army Corps of Engineers, Washington, DC.

Van Asselt, M.B.A., Rotmans, J., 2002. Uncertainty in integrated assessment modelling – from positivism to pluralism. Climatic Change 54, 75-105.

Wheaton, J.M., Pasternack, G.B., Merz, J.E., 2004a. Spawning habitat rehabilitation - 2. Using hypothesis development and testing in design, Mokelumne River, California, U.S.A. International Journal of River Basin Management 2 (1), 21-37.

Wheaton, J.M., Pasternack, G.B. and Merz, J.E., 2004b. Use of habitat heterogeneity in salmonid spawning habitat rehabilitation design. In: D.G.d.J. Lastra and P.V. Martinez (Editors), Fifth International Symposium on Ecohydraulics, Aquatic Habitats: Analysis & Restoration, Madrid, pp. 791-796.

White, J.Q., 2008. Valley width controls on riffle location and persistence on a gravel bed river. M.S. Thesis, Department of Hydrologic Sciences, University of California, Davis.

Whittaker, J.G., Jaeggi, M.N.R., 1982. Origin of step-pool systems in mountain streams. Journal of the Hydraulics Division ASCE 108, 758-773.

Wilcock, P.R. and Southard, J.B., 1988. Experimental-Study of Incipient Motion in Mixed-Size Sediment. Water Resources Research, 24(7): 1137-1151.

Wilcock, P.R., Barta, A.F., Shea, C.C., Kondolf, G.M., Matthews, W.V.G., Pitlick, J.C., 1996. Observations of flow and sediment entrainment on a large gravel-bed river. Water Resources Research 32, 2897-2909.

Williams, G., Wolman, M.G., 1984. Downstream Effects of Dams on Alluvial Rivers. Professional Paper, Vol. 1286, U.S. Geological Survey, Washington, DC.

Wolman, M.G., 1954. A method of sampling coarse river-bed material. Transactions of the American Geophysical Union 35, 951-956.

Woodsmith, R.D. Hassan, M.A., 2005. Maintenance of an obstruction-forced pool in a gravel-bed channel: streamflow, channel morphology, and sediment transport. In: Garcia, C., Batalla, R.J. (Eds.), Catchment Dynamics and River Processes: Mediterranean and Other Climate Regions. Development in Earth Surface Processes, Vol. 7, Elsevier, Amsterdam, The Netherlands, pp. 169-196.

FIGURES

Fig. 1. Map and aerial photo of the Yuba River showing the location of the study site in Timbuctoo Bend below Englebright Dam.

Fig. 2. Typical annual hydrographs for the (A) unregulated period (1904-1942), (B) post-Englebright Dam period (1942-1971), and (C) post New Bullards Bar construction (1971-present). Actual water years shown are 1922, 1950, and 1991, respectively.

Fig. 3. Photographs of the same downstream 1-km straight-away in Timbuctoo Bend taken in (A) 1906 by G.K. Gilbert and (B) 2006 by the authors illustrating incision on the order of 15 m and persistence of similar morphological units.

Fig. 4. Topographic map of the wetted channel at the study site at 23.4 m^3s^{-1} prior to the May 2005 flood showing the cross section locations where depths and velocities were measured (XS1, XS2, and XS3) as well as locations of cross sections for hydraulic geometry analysis (pool, riffle, and run).

Fig. 5. Hydraulic geometry relationships: WinXSPRO results compared to FESWMS results.

Fig. 6. FESWMS velocity magnitude results for all discharges: (A) summer low flow (23.4 m^3s^{-1}), (B) present-day Q_b (159.2 m^3s^{-1}), (C) pre-Bullards Bar Dam Q_b (328.5 m^3s^{-1}), and (D) and a 7.7 year event (1215.8 m^3s^{-1}).

Fig. 7. (A) Depth and (B) velocity validation best fit curves for three cross sections, see Fig. 4 for cross section location.

Fig. 8. Simplified visualization of DEM difference illustrating areas of scour (shades of red or in b/w: shaded dots) and deposition (shades of blue or in b/w: shaded hatch marks) by morphological unit. Locations indicate (1) pool scour, (2) upstream knickpoint migration, (3) bedrock outcrop constriction corresponding to scour, (4) side channel deposition, (5) island/bar complex elongation by deposition, and (6) deposition on willow levee and floodplain.

Fig. 9. Box and whisker plot of 2D model predicted Shields stress data related to the occurrence

of scour (elevation change < -0.15 m), no change (-0.15 m < x < 0.15 m), and deposition (> 0.15 m) on a point-by-point basis.

Fig. 10. Comparison of 2D-model predicted τ^* for the flood peak discharge and elevation change 2004-2005 stratified by bankful wetted cross sections and the floodplain. Shaded area is region of uncertain channel change.

Fig. 11. Cross sections from 2004 to 2005 showing locations of scour and deposition with corresponding 2D model output Shields stresses for (A) pool, (B) riffle and (C) run cross sections. View is looking upstream.

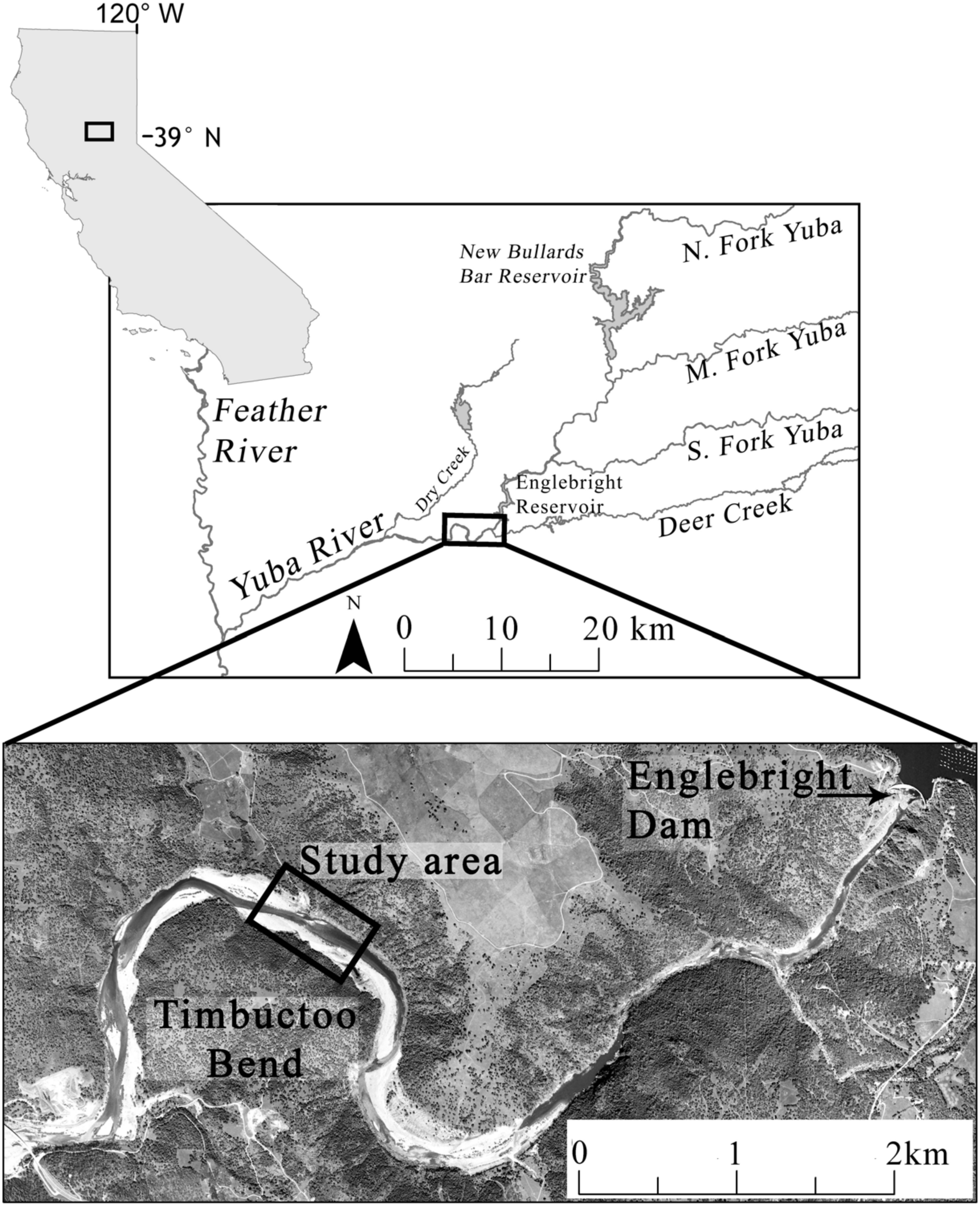

120° W
39° N
New Bullards
Bar Reservoir
N. Fork Yuba
M. Fork Yuba
S. Fork Yuba
Feather
River
Dry Creek
Englebright
Reservoir
Deer Creek
Yuba River
N
0 10 20 km
Englebright
Dam
Study area
Timbuctoo
Bend
0 1 2km

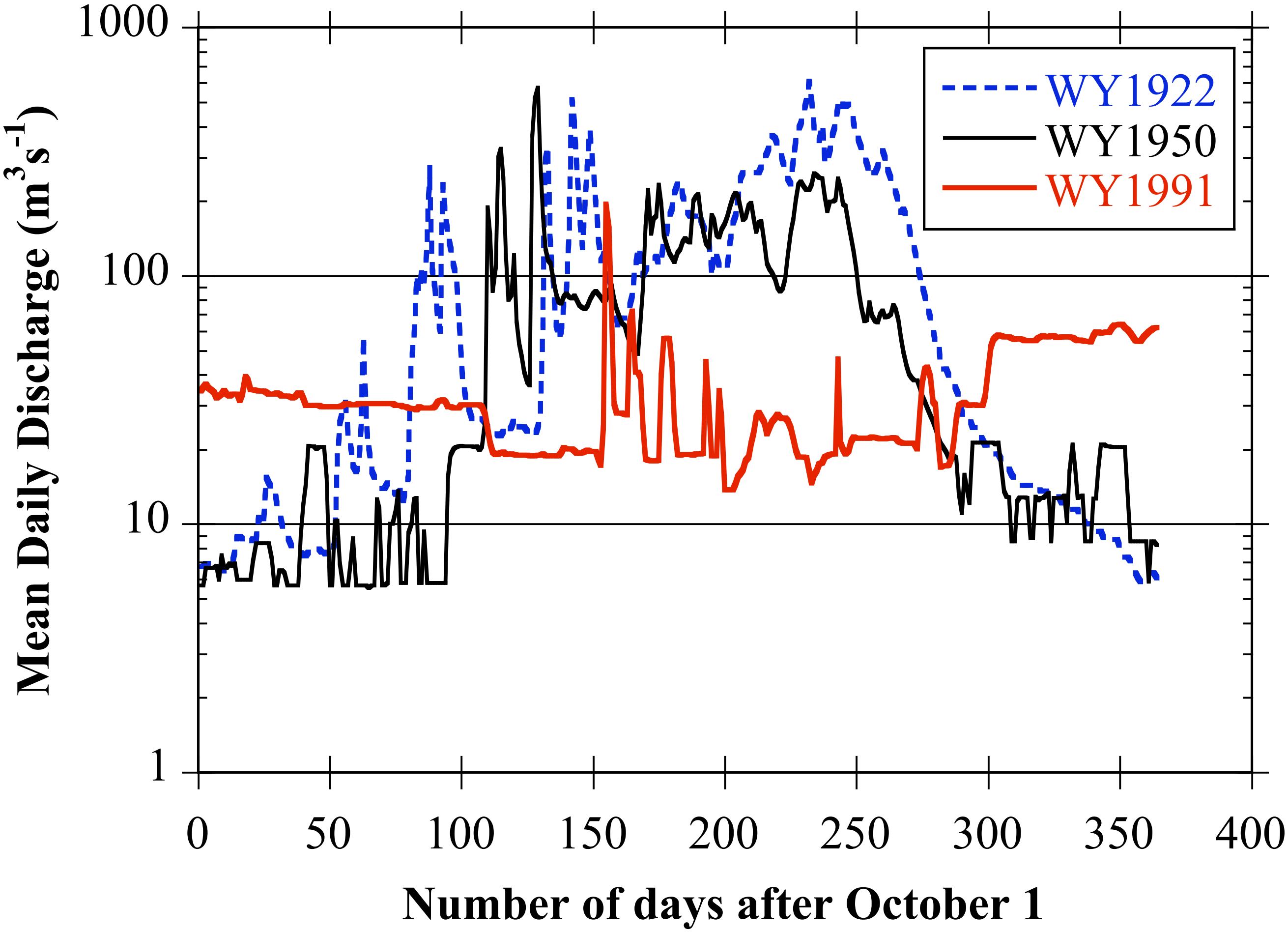

WY1922
WY1950
WY1991
1000
100
10
1
Mean Daily Discharge (m3s-1)
0
50
100
150
200
250
300
350
400
Number of days after October 1

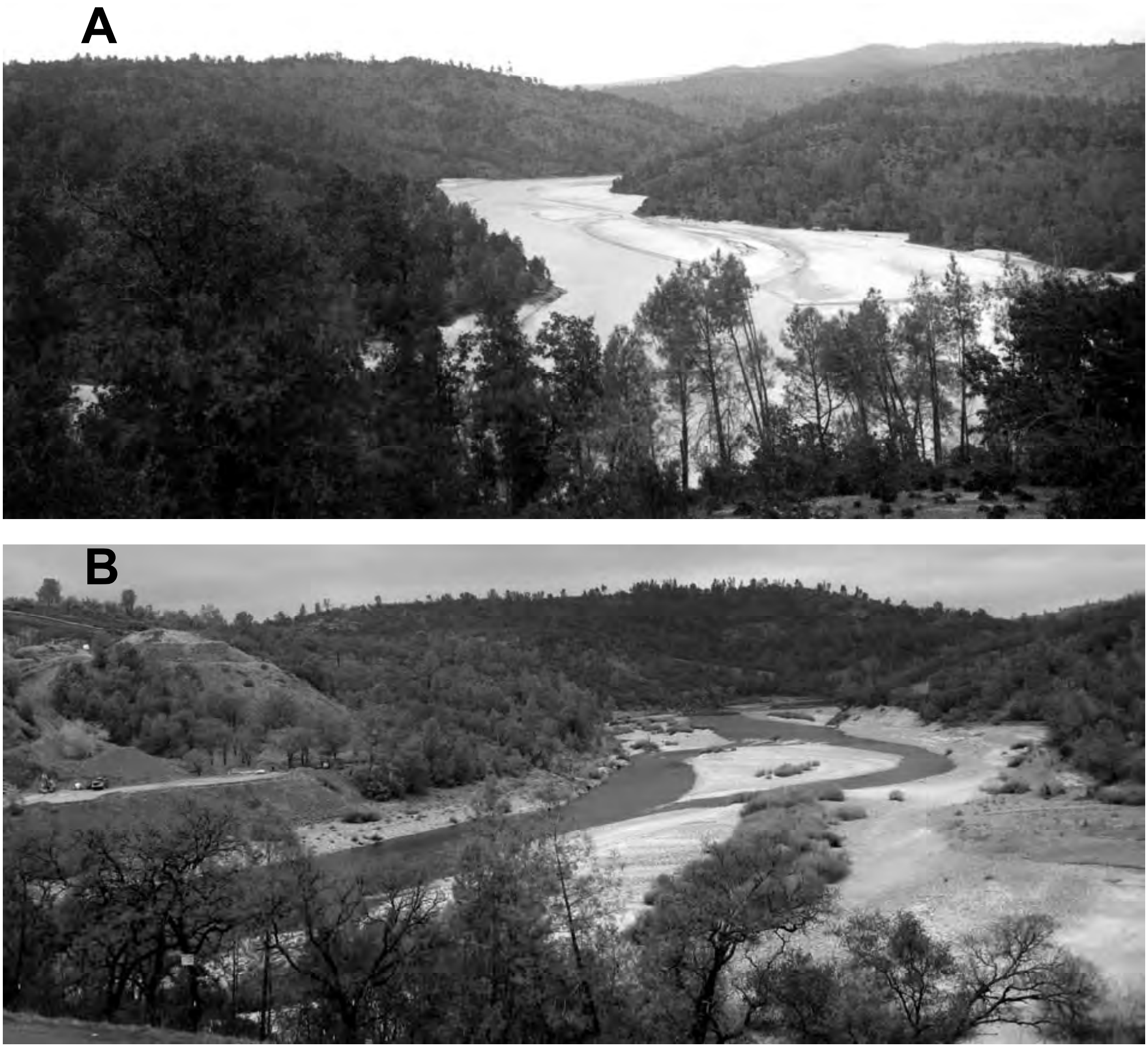
A
B

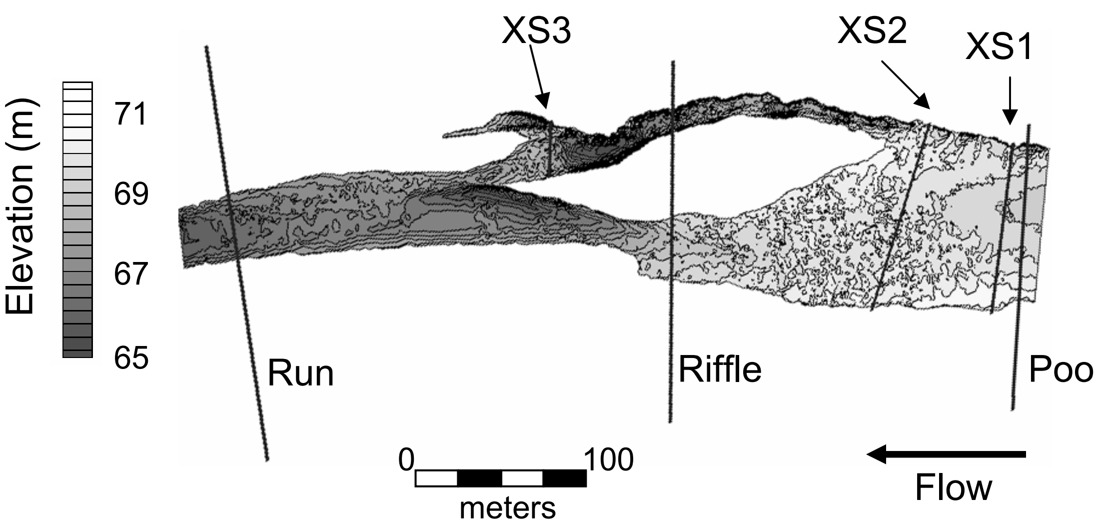

Elevation (m)
71
69
67
65
XS3
XS2
XS1
Run
Riffle
Pool
0
100
meters
Flow

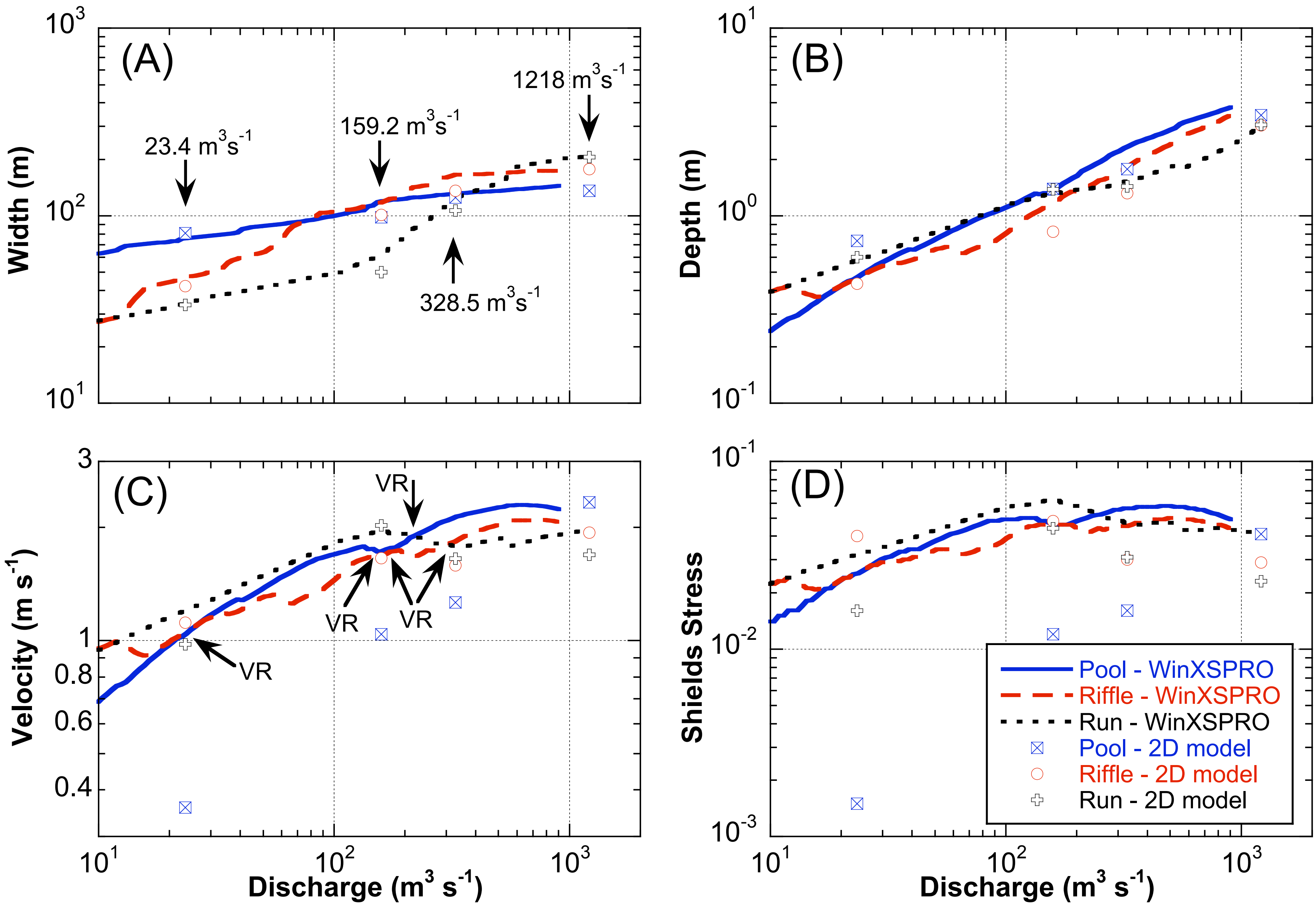
(A)
Width (m)
23.4 m3s-1
159.2 m3s-1
1218 m3s-1
328.5 m3s-1
(B)
Depth (m)
(C)
Velocity (m s-1)
VR
(D)
Shields Stress
Discharge (m3 s-1)
Pool - WinXSPRO
Riffle - WinXSPRO
Run - WinXSPRO
Pool - 2D model
Riffle - 2D model
Run - 2D model

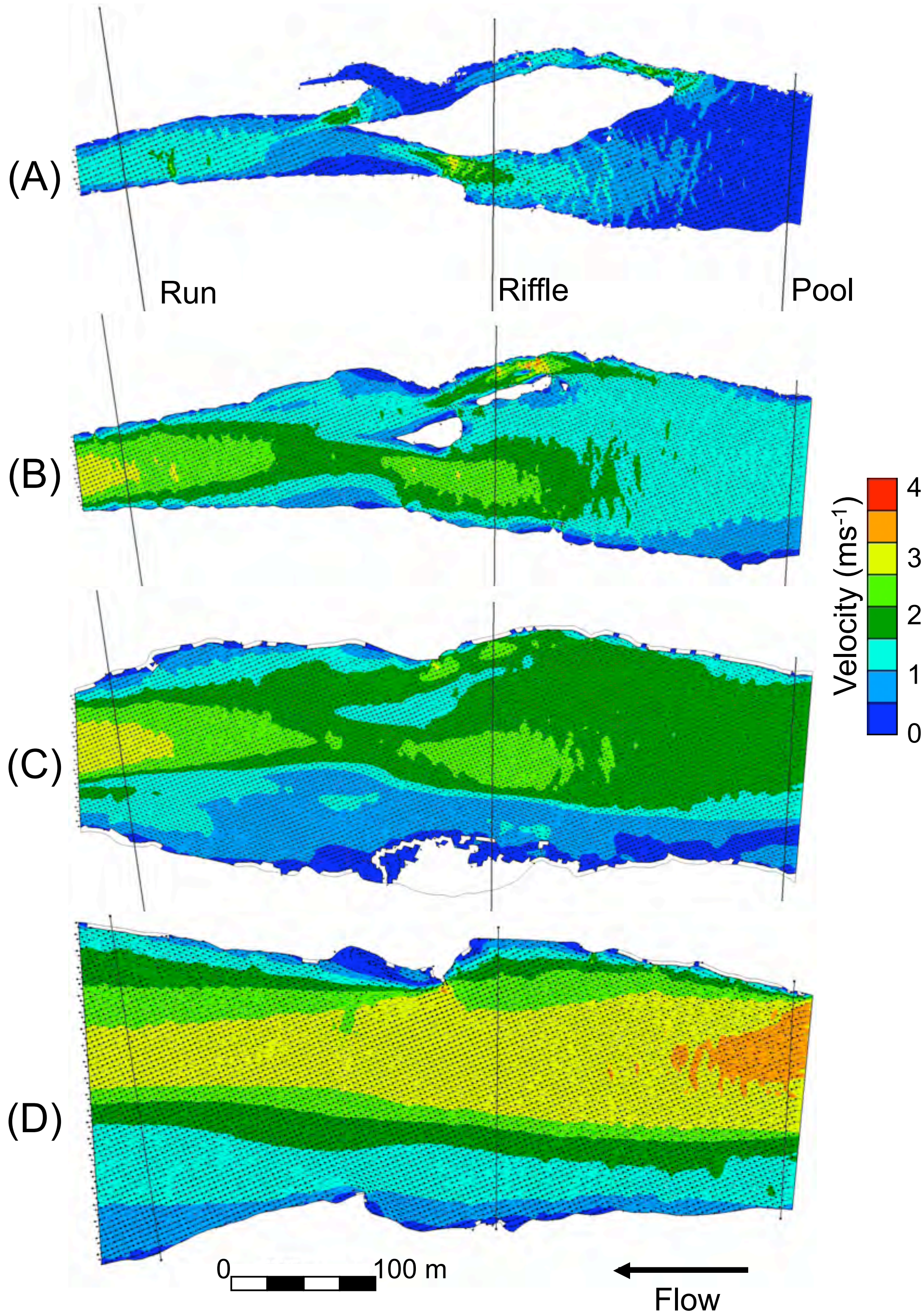
(A)
Run
Riffle
Pool
(B)
(C)
(D)
Velocity (ms-1)
4
3
2
1
0
0
100 m
Flow

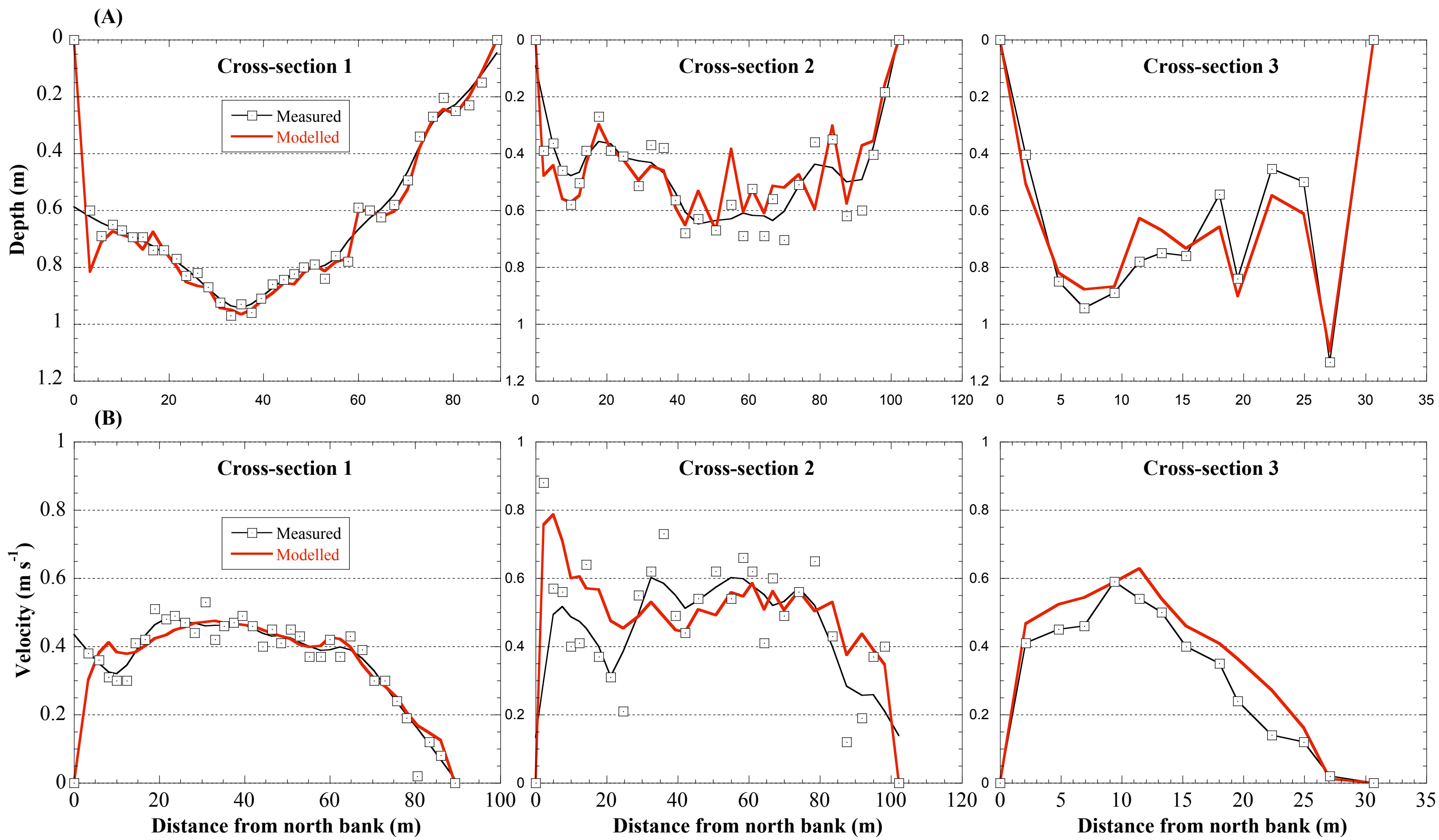
(A)
Cross-section 1
Cross-section 2
Cross-section 3
Measured
Modelled
Depth (m)
(B)
Velocity (m s-1)
Distance from north bank (m)
Distance from north bank (m)
Distance from north bank (m)

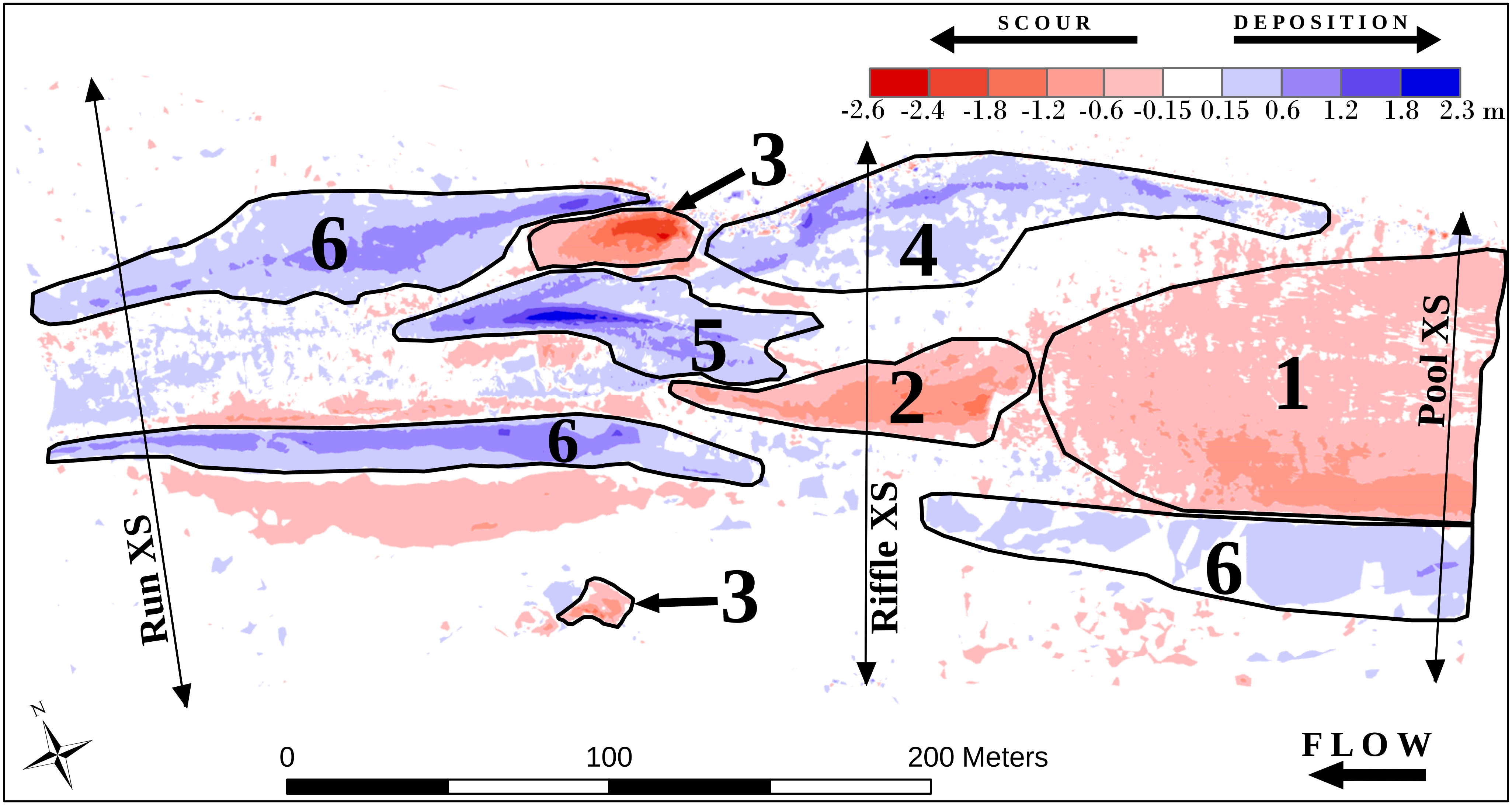
SCOUR
DEPOSITION
-2.6 -2.4 -1.8 -1.2 -0.6 -0.15 0.15 0.6 1.2 1.8 2.3 m
Run XS
Riffle XS
Pool XS
1
2
3
3
4
5
6
6
6
N
0
100
200 Meters
FLOW

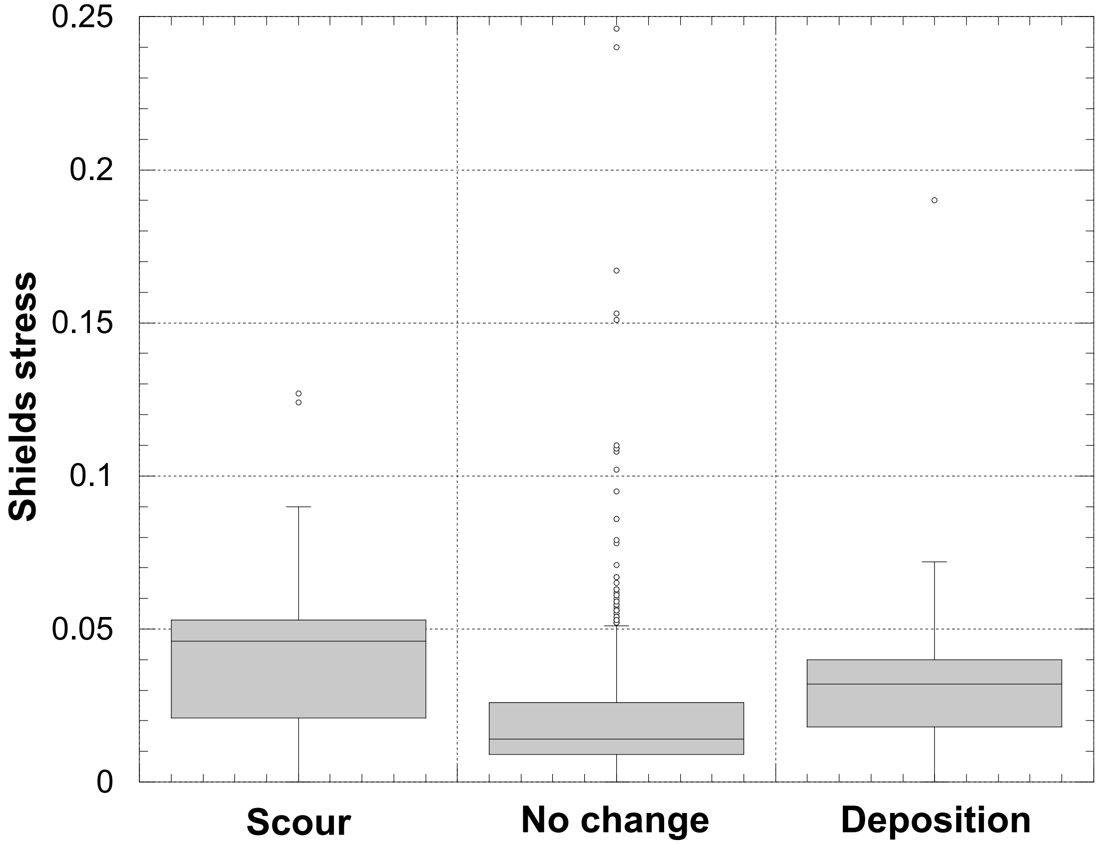

Shields stress
0.25
0.2
0.15
0.1
0.05
0
Scour
No change
Deposition

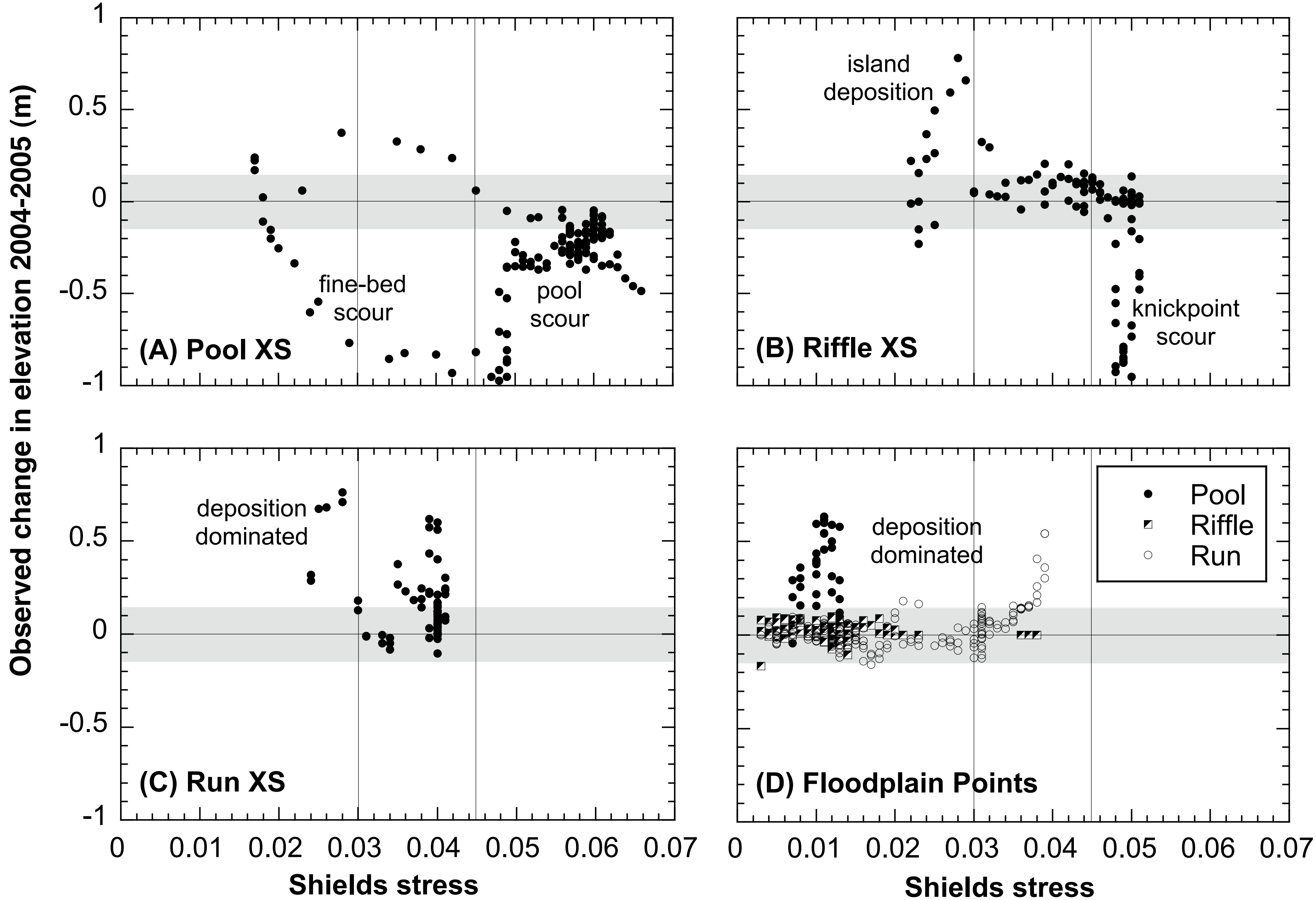

Observed change in elevation 2004-2005 (m)
Shields stress
(A) Pool XS
fine-bed scour
pool scour
(B) Riffle XS
island deposition
knickpoint scour
(C) Run XS
deposition dominated
(D) Floodplain Points
deposition dominated
Pool
Riffle
Run

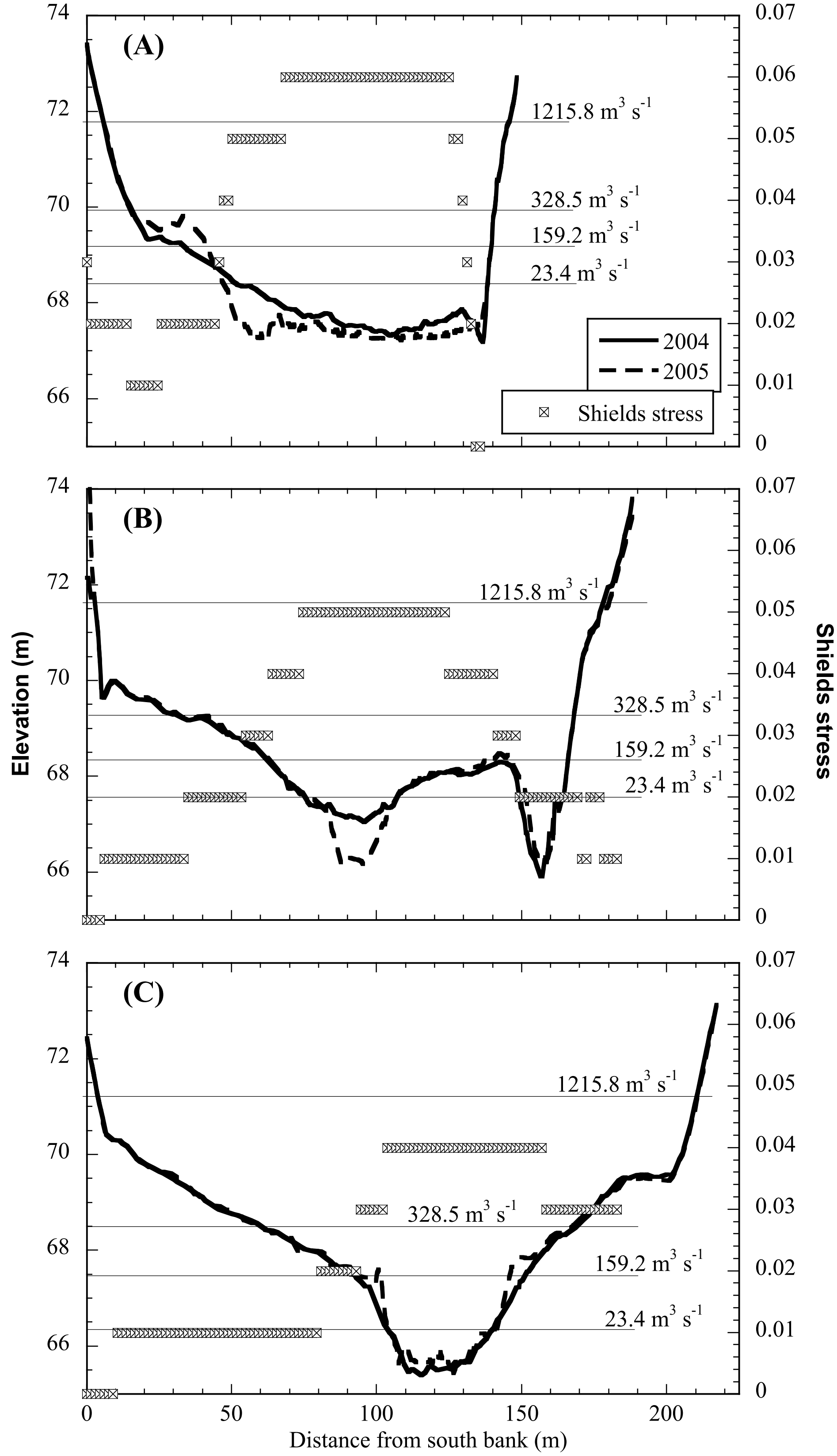

(A)
(B)
(C)
1215.8 m^3 s^{-1}
328.5 m^3 s^{-1}
159.2 m^3 s^{-1}
23.4 m^3 s^{-1}
2004
2005
Shields stress
Elevation (m)
Shields stress
Distance from south bank (m)
74
72
70
68
66
0.07
0.06
0.05
0.04
0.03
0.02
0.01
0
0
50
100
150
200